HP
JAESR2025
Hummingbird Publications
Journal of Agricultural & Env. Sci. Research
www.hummingbirdjournals.com
© May, 2025
Vol. 8 No. 1

Preliminary Investigation for Groundwater Exploration using Electromagnetic Method of Terrain Conductivity Variation in Papalanto, South-West Nigeria

Ishola S.A

Department of Earth Sciences, Olabisi Onabanjo University Ago-Iwoye, P.M.B 2002, Ago-Iwoye, Ogun State, Nigeria

Corresponding Author: *ishola.sakirudeen@oouagoiwoye.edu.ng*

DOI: https://doi.org/10.70382/hujaesr.v8i1.027

Keywords: Terrain, Dipole Moment, Probing Depth, Fissures, Frequency Domain.

Abstract

Papalanto District is a typical sedimentary formation within Dahomey basin where ground conductivity measurements were undertaking with Geonics EM 34-3 along 5 traverses with profile lengths varying between 160 and 200m. Comprehensive geophysical fieldworks were done adopting Frequency Domain Electromagnetic Method (FDEM) to ascertain both the vertical and lateral variations of subsurface conductivity probing depths of 20 m, 40 m and 60 m seeking different investigated depth. The EM data were acquired at 500 m intervals along 10 profiles. The Vertical Dipole Moment (VDM) in the first layer exhibited the highest and lowest true conductivity of 134.31 and 78.9 mmho/m for EMIPAP1 and EMPAP6 respectively and the corresponding Horizontal Dipole Moment (HDM) exhibited the highest and lowest true conductivity values of 1141.92 and 118.0 mmho/m for EMPAP5 (2^{nd} layer) with depth of 9m in HDM and 14m in VDM and EMPAP1 (1^{st} layer) respectively. Lowest true conductivity values of 84.55 and 122.0 mmho/m were recorded in the second layer for VDM and HDM respectively. The highest recorded true conductivity values in the first layer were 133.33 mmho/m (EMPAP1) and 167.48 mmho/m in EMPAP7 (depth 7.8m in HDM and 9.2m in VDM) respectively. The highest depth of penetration respectively recorded for HDM and VDM in the first layer were 33m in EMPAP10 and 14m in EMPAP1 and EMPAP2 while the lowest depth of penetration respectively recorded for HDM and VDM in the first layer were 2m in EMPAP3 alongside EMPAP6 and 6.5m in EMPAP8 as the depths of penetration remained indeterminate in the second layer due to current termination. The appreciable variation in conductivity with recognizable positive peaks and broad bowl shaped anomalies observed in the high conductivities in both orientations is a resultant effects of weathering of the subsurface geological horizon and are possible indications of the vulnerability of its subsurface hydrogeological environment to invasion of contaminant seepages and consequent pollution of the investigated locations of the study area. The qualitative interpretation of EM results identified areas of hydrogeologic importance and forms a predictive and suggestive basis for Vertical Electrical Sounding (VES) investigation; points of positive EM anomalies were considered as priority area for prospective groundwater development necessitating more advanced groundwater exploration techniques.

Introduction

The acquisition and interpretations of Electromagnetic method (EM) seem difficult because of the varying subtility and inherent inhomogeneities of the subsurface coupled with the abrupt changes in lithology, variable thicknesses, and electrical properties of weathered layer and bedrock materials. Pathway to the nature and conditions of the earthcrusts is basically one of the most difficult challenge ever encountered by earth scientists because it is principally based on what can be observed per time and how better observers can perceive, predict and interpret his observation (Alabi et al., 2019; Ishola *et al.,* 2023). Groundwater has been a mysterious nature's hidden and endowed resources that must explored for effective utilization and maximization by the society (Ishola *et al.,* 2023). Daily exploitation of groundwater has continued to maintain a significant concern at every point in time due to its unavoidable demands by all and sundry; streams, rivers ponds, lakes among other sources, none naturally possesses a high level of sanitary integrity as groundwater because groundwater served and has been serving as excellent natural resource free of microbial loads and generally possess chemical quality of its domain qualifying it for most domestic and industrial utilization (Macdonald *et al.,* 2002).

Terrain conductivity variations are crucial in preliminary groundwater exploration because they can indicate areas with higher groundwater potential. Conductivity surveys like the electromagnetic method help to identify zones with fractured or fissured rock formations and interconnected joints which often favour groundwater accumulation y providing broad overview of subsurface conditions, guiding more detailed study. These areas can then be further investigated with methods like vertical electric sounding (VES) to pinpoint optimal well locations (Aly et al., 2018; Okpoli and Ozomoge, 2019; Tyoh et al., 2025; Huang et al., 2022). Terrain conductivity meters are cost effective and can provide a large amount of data quickly making them ideal starting point for groundwater exploration (Azmy et al., 2023).

One of the significant assistant that exploration activities have offered earth scientists most notably the applied geophysicists is the detailed understanding of the earth interiors in terms of nature, properties, resources and their individual responses to measurable quantities in the field. The primary aim and objectives of applied geophysical investigations are detection, investigation, and drawing line of inferences on the existence, location and extent of underground water, ore minerals, solid minerals, hydrocarbons, geothermal reservoirs, radioactive deposits among others and subsurface geological structures that are connected with them using surface techniques for the measurement of the physical parameters of the earth alongside with the encountered anomalies in these measured parameters (Alisa, 1990). EM method of geophysical prospecting provides a relatively fast approach to detecting and delineating fractures and where this delineated fractured zone possesses high conductivity; it could be inferred as mineralization zones or aquiferous zones (Benson, *et al.,* 1997; Onwuegbuchulam *et al.,* 2016; Ishola et *al.,* 2023). Therefore, a detailed geophysical investigation and hydrogeological understanding of the subsurface conditions in terms of aquifer types and their spatial location are not only necessary but they are basic requirement for efficient characterization of aquiferous zone and ultimate unraveling the hidden and seemingly mysterious nature of this endowed resources called groundwater (Ishola *et al.,* 2023).

The study area is located within the sedimentary part of Southwestern Nigeria and transits largely into the sediments of the Dahomey basin. The subsurface geophysical investigation adopting (EM) conductivity measurement was carried out in the study area for groundwater prospecting. Electromagnetic profiling is a widely used geophysical technique effective in the delineation of overburden rock formation and clay regolith as well as in the detection of fissured media and zones of deep connection to subsurface weathering of the consolidated sedimentary terrains (Beeson, *et al.,* 1988., Hazell, *et al.,* 1988, Olayinka, 1990, Olayinka, *et al.,* 2004; Ishola *et al.,* 2023). In numerous geophysical episodes, reconnaissance EM surveys have been utilized in the detection and exploitation of aquiferous zones and their accompanied features namely faults, fractures, and joints (Ishola *et al.,* 2023). Geophysical methods perform unending notable tasks in sourcing for suitable and productive groundwater reservoirs (Ishola *et al.,* 2021). Electrical resistivity method has been routinely utilized in field exploration for groundwater. However, several other geophysical methods have been successfully applied either as a single technique or in composite approach for field prospecting for groundwater resources in varying geologic environment. The electromagnetic method has proven not only as a very useful technique but also its suitability groundwater investigation in both sedimentary and basement terrains, most especially as a reconnaissance tools in the hands of exploration field professionals to understanding the nature and groundwater development feasibility studies of any encountered aquiferous zone (Worthington, 1977. Palacky *et al.,* 1981; De Jong et al., 1981; Amadi and Nurudeen, 1990; Olorunfemi *et al.,* 2001; Egwebe *et al.,* 2004; Ariyo *et al.,* 2009; Okafor and Mamah, 2012; Ishola, 2019; Ishola *et al.,* 2021; Ishola *et al.,* 2023). The principal advantage of the EM- methods that has withstood the test of time is that direct contact with the earth surface is not in any way required when compared to Direct Electrical methods (Ishola *et al.,* 2023**).** Therefore, the field performance of EM- measurement can be rapidly and simply done than wnen the DC measurement is utilized for the same task rendering it a high and very relevant technique for rapid assessment studies in line with other presumably fast and accurate techniques. EM does not register any individual outcome from field reading the difference from adjacent readings are significant and subsurface picture is equally built based on all the acquired readings along the survey line and adjacent lines of investigation (Ishola *et al.,* 2023). Also, Electromagnetic method can be utilized alone or in integrated form with other exploration geophysical techniques such as gravity, electrical resistivity, seismic refraction, reflection seismology, induced potential methods in the course of sourcing for groundwater which is a function of the scope of prospecting whether it is on local scale or a regional coverage. This study is basically centered on groundwater using by the interpretation of the observed conductivity variation where subsurface site information on the hydrogeologic framework of the encountered aquifer units, and delineation of fractured/weathered zones for subsequent drilling and installation water wells in the study area.

STUDY AREA

The study area is discussed under Existence, Location and Accessibility, Climate, Vegetation, Drainage and Geology in this section.

Existence, Location and Accessibility

The entity called Ewekoro Local Government Area (LGA) where the study area belongs first came into existence on 22nd of May, 1981. It lies within Ogun State, South-West Nigeria; which is bounded in the West by Benin Republic, in the south by Lagos State, in the north by Oyo and Osun States, and in the east by Ondo State. In 1984 when the military took over, the region was considered for restructuring. So, it was merged with Ifo Local Government in 1989 (Ishola, 2019). However, on December 16, 1996 Ewekoro Local Government was restored as an autonomous Local Government by the then Federal Military Government alongside five others in the state, thus increasing the number of Local Government in Ogun State from fifteen to twenty. Papalanto area is bounded by longitude $3^{o}13^{1}$E and latitude $6^{o}54^{1}$N; it harbours one of the largest outcrops of Ewekoro limestone that easily attracts attention. It extends from Ibesse, 4km east of Papalanto along Papalanto-Shagamu road to Ogun River, 5km east to Iro community (Ishola, 2019). It occupies a total area of 16,400 km^2 with a population of 255,156 at 2006 population Census and a postal code area of 112 with an average elevation of 64m above sea level. The area is mildly densely populated with 297 people per km^2 with the nearest town larger than 50,000 inhabitants takes about 0:15 hour by local transportation. The indigenous dwellers of Ewekoro Local Government area are mainly the Egbas, particular the Egba Owus. The people engage primarily in farming and trading activities. The area is essentally in rural settlement (Ishola, 2019). The climate is not different from that of these towns and villages earlier mentioned and adjoining towns such as Ifo, Sagamu and others. However, the advent of West African Portland Cement Company (WAPCO) changed the economic sphere of this once sleepy and serene town (Ishola, 2019). The Ewekoro cement production facility of the WAPCO established in 1959 is the oldest cement factory in Nigeria. Although quality limestone has been discovered in this settlement since the colonial period, mining and quarrying did not commence until early 70s when attempt were made to mine and export. However as a follow up to the first and second National development plans, the company was established with Larfage of France being the major technical partner. The company has since being privatized. The annual cement production from the factory using wet and semi-wet clinker production technology varied between 254,000 and 479,000 metric tonnes (WAPCO, 2000). Fig. 1 shows the geological map of the Study Area within the Nigerian Part of Dahomey Embayment (Modified by Ishola, 2019). Figure 2 Displays the GoogleEarth imagery of the selected Investigated study area within in Ewekoro LGA, the map of Ogun State showing the geology of the study areas is presented in Figure 3, the inset map showing political divisions of the study area within Nigerian continental environment is shown in Figure 4, the map showing the selected investigated locations in the study area is shown in Figure 5 while Figure 6 the accessibility of the study areas amidst the investigated points in Ewekoro LGA. The entire study area is generally accessible by major roads and several footpaths, although the road from Abeokuta town to the investigated area is tarred. In addition to Ewekoro-Papalanto road, the survey locations can equally be accessed through a major road from Lagos State through Sango-Ifo express road (Kehinde-Phillips, 1992; Ishola and Gbadebo, 2024).

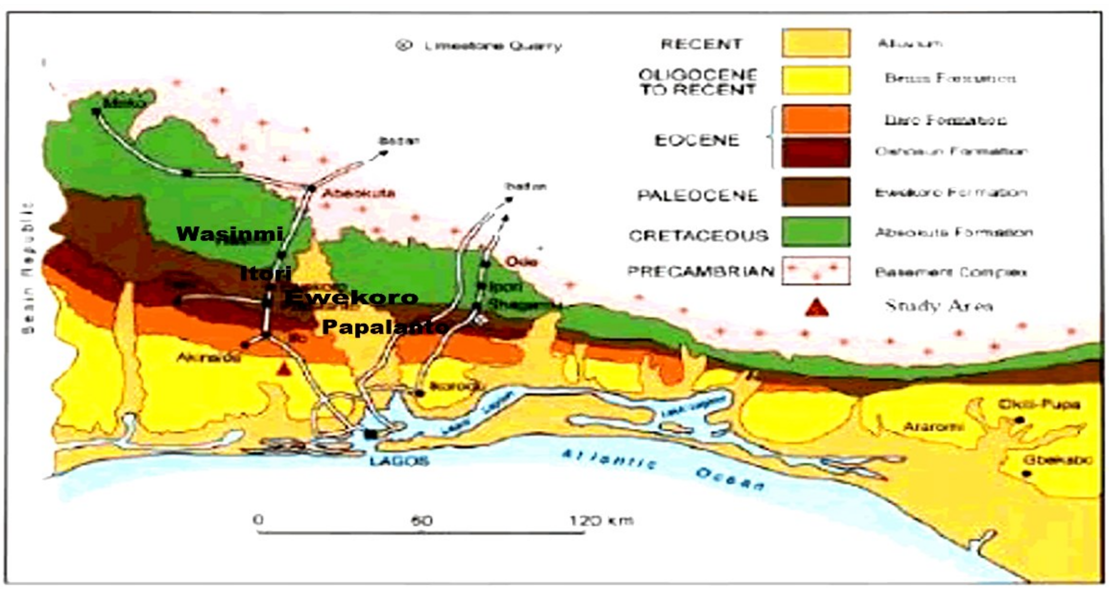

Figure 1: Geological Map Showing the Selected Locations of the Study Area within the Nigerian Part of Dahomey Embayment (Billman, 1992; modified by Ishola, 2019).

Figure 2: Display of GoogleEarth imagery of the selected Investigated study area within in Ewekoro LGA, South-West Nigeria (Ishola *et al.,* 2024).

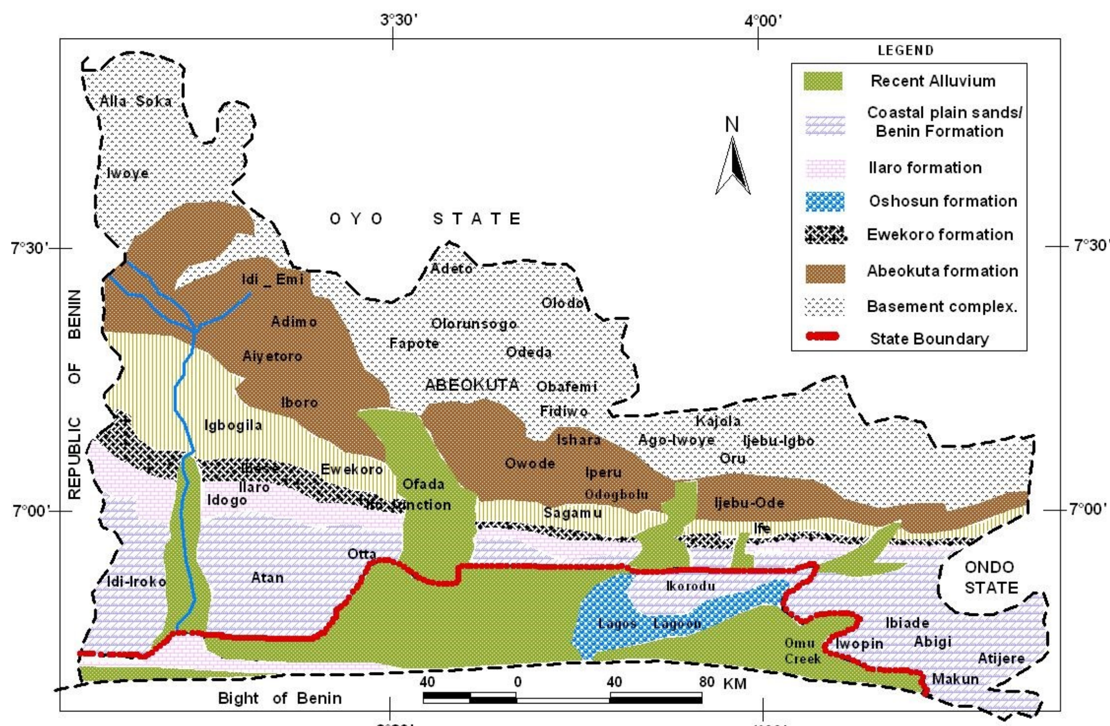

Figure 3: A Map of Ogun State showing the Geology of the Study Areas after Kehinde-Phillips (1990); Obiora and Onwuka (2005)

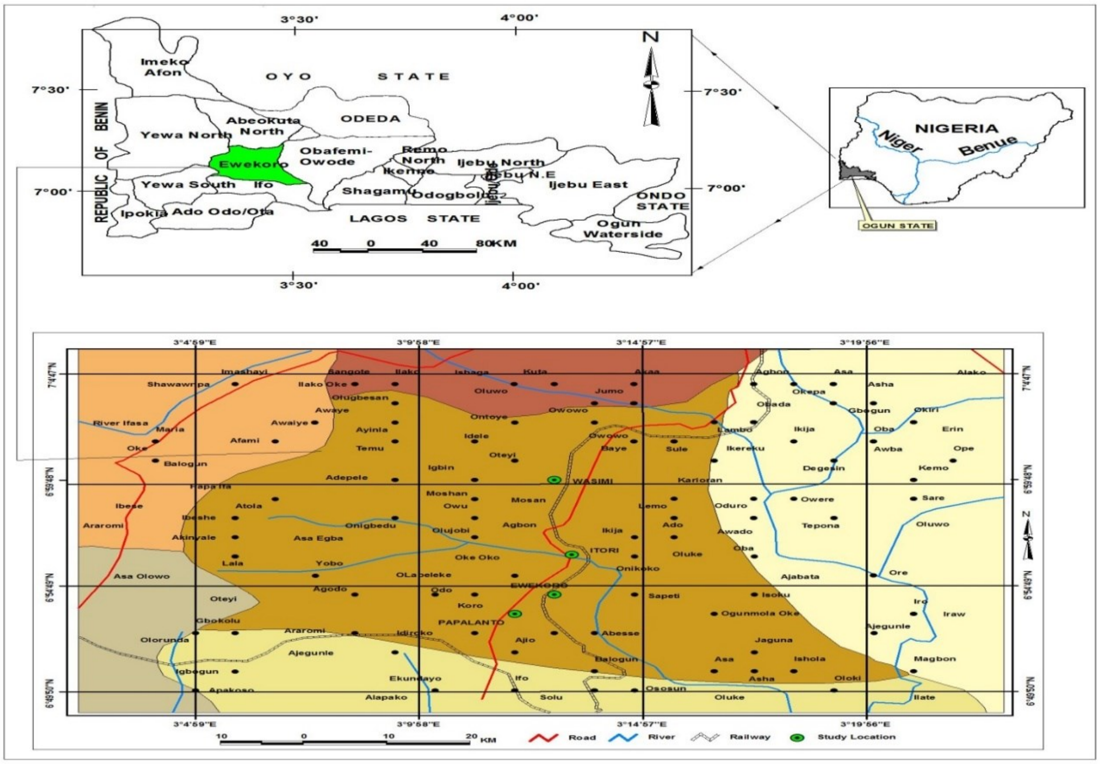

Figure 4: Inset Map showing the Study Areas in Ogun State within Nigeria Continental Domain (using Esri Data/Nigeria Political Information in Arcview GIS 3.2A Environment)

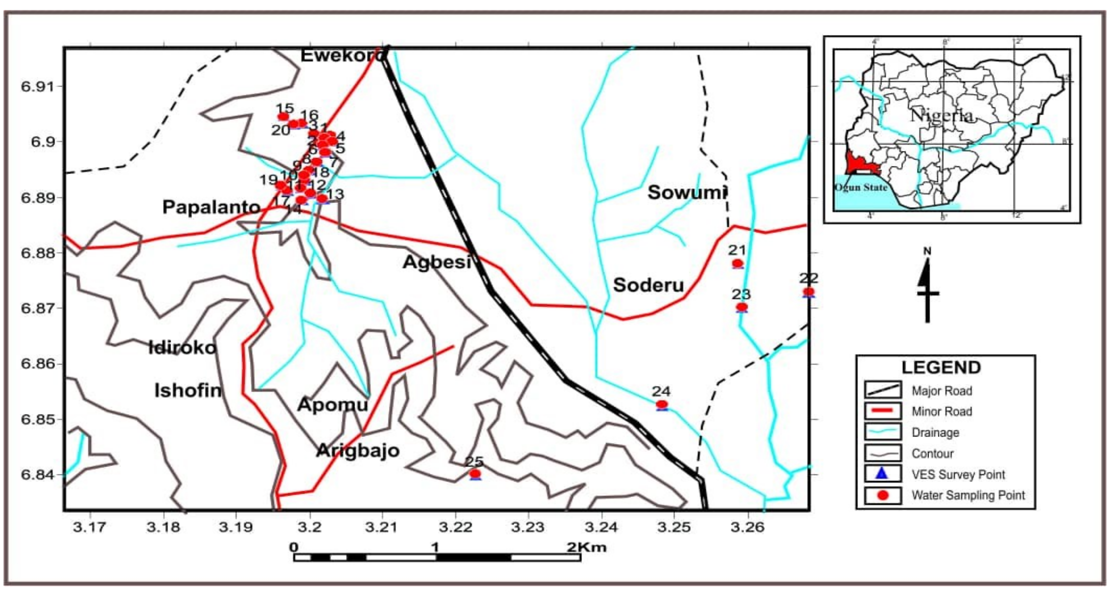

Figure 5: Data Acquisition Map showing the Investigated Locations in Papalanto Study Area in Ewekoro LGA, South-West Nigeria (Ishola *et al.,* 2024).

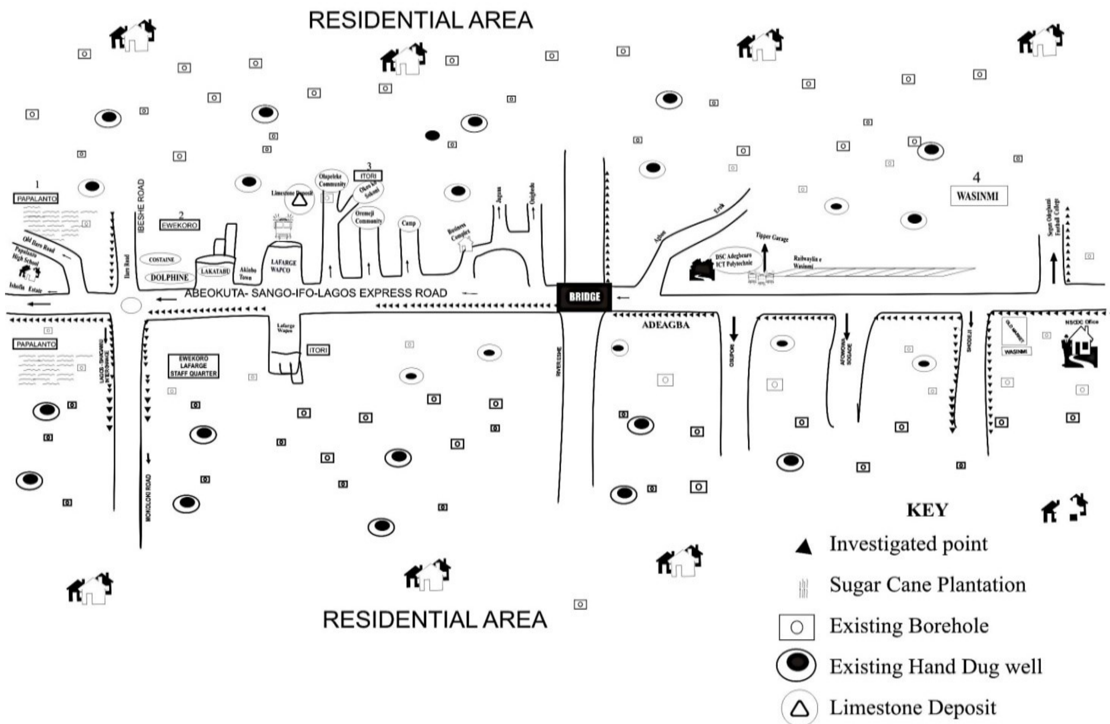

Figure 6: Location and Accessibility of the Investigated Points in Ewekoro LGA (Ishola *et al.,* 2024).

Weather, Climate and Environmental Hazards Prediction

The study areas is generally a low lying to gentle undulating terrain that falls within the humid tropical climate characterized by two distinct seasons predominant in the tropics in the southern part of Nigeria namely, the wet and dry seasons. The wet season usually occur from March to October, the climate is dominated by the tropical maritime airmass or moisture laden Southwest winds from the Atlantic Ocean that produces heavy rainfall; most of the rainfall comes in torrential showers resulting in high run-off while the dry season occurs from November to late February or early March under the influence of the dry continental airmass or North-Easterly winds from Sahara desert. The little dry season in the mid-west season of July/August months is dominant in the area (Oguntoyinbo, 1978; Gbuyiro *et al.,* 2002). The harmattan season, a season of dusty high winds, unusual cold and extremely dry conditions, lasts from November to February. It is caused by the tropical continental air from the Sahara Desert which displaces the tropical Maritime air from the Gulf Guinea (Olayinka, 2000). Ewekoro has no distinct temperature seasons; the temperature is relatively constant during the year. The

wet season ensures adequate supply of water and continuous presence of moisture in the air. Hence, the study area experiences high diurnal and annual temperature, lack of cold season, high precipitation, low pressure, high evapotranspiration and high relative humidity (Gbuyiro *et al.,* 2002; Omogbai, 2010). The temperatures at night are cooler than during the daytime. November is an average, the month with most sunshine. February is the warmest with an average monthly temperature of 33.5°C at noon. August is coldest with an average temperature of 21.9°C. Rainfall and other precipitation peaks around June. The time around January is the driest.
The study area has a mean annual temperature of 27°C in July and 32°C in February, and the average monthly temperature of 25.7°C. It has relative high humidity of 71.09 % and long wet season that ensures adequate supply of water and continuous presence of moisture in the air. The annual rainfall is estimated to be 1194.33mm (Gbuyiro *et al.,* 2002 and WAPCO, 2000). Cold and hazy conditions are usually prevailing especially towards the end of the year while hot and dusty conditions are experienced during dry season. Hence, the study area is characterized by high diurnal and annual temperature, high precipitation, low pressure, high evapo-transpiration and high relative humidity. The major water bodies in the region are Yewa and Ogun rivers which flow into Lagos lagoon while their tributaries are found in Ewekoro Local Government Area as Alaguntan River, Akinbo River and Eshe River. There are however streams running parallel in the area. Also ponds are not left out. Due to the alternation of wet and dry seasons, the water table fluctuates in response to the seasonality of rainfall. During the wet season, groundwater level rises towards the surface and drops as the dry season sets in.
In terms of environmental hazards, the following parameters 20%, 70%, 70%, 0%, 0%, 0% for Earthquake, Flood, Drought, Landslides, Volcano and Cyclone have been estimated and predicted in their respective order in Ewekoro. Ewekoro can have low impact or less earthquakes (on the average of one every 50 years) with occurrences at < 5 Richter. There is a medium to high occurrence of periods with extreme drought. Flooding risk is medium high although, during the wet season, parts of the city become flooded as a result of heavy rainfall, low relief, high tides and poor structural planning of buildings and drainage facilities (WAPCO, 2000; WAPCO, 2001; Ishola, 2019).

Natural Vegetation and Site Description

The natural vegetation of Ogun State which the study areas belong consists of the forest and the savanna which affect the floristic composition of the plant communities. The forest vegetation is of two types, namely, the fresh water swamp forest and the lowland rain forest. The savanna found in the State is mainly of the derived savanna type. The rainforest vegetation is typified by perennial trees which may vary in height forming storey with characteristics thick vegetation due to high rainfall. The vegetation changes with seasons with the incoming of the rains, the green grasses are back to life and the foliage of the trees becomes green and thick. Where the soil is wet due to river drainage denser fringing forest are found. During dry season some of the trees, which develop umbrella shaped canopies shed their leaves in order to minimize loss of water by transpiration (Ayedun *et al.,* 2013; Ishola, 2019). Human activities on the natural vegetation have reduced the original forest to secondary forest bush, regrowth and thickets. One very important impact of the quarry is deforestation. This simply means the loss of vegetation cover that is necessitated by the need to move equipments to the site, removal of the topsoil or (overburden) stemming of explosives and removal of blasted limestones. These effects are normally reduced by appropriate mitigating actions such as massive reclamation of the mined areas using new overburden materials and a forestation programme that involve planting of varieties of trees that have ornamental values, that can hold the soil structure well and could cover the exposed land well. Limestone mining in Ewekoro had resulted into the conversion of many farmlands and settlements into quarry sites. The house types on the site are mainly the makeshift type built for use on no permanent basis. The few landowners on the factory site are resident on site to participate in cement business and no longer to farm as it was before now.

Topography and Drainage pattern

Ogun State which the study areas belong is drained by many big perennial rivers that are consequent in nature and numerous obsequent streams. The rivers include Ogun, Oshun, Yewa, Opebi, Yemoji and Ore with Ogun River being the dominant one in the study areas which runs across it from north to south (Ishola, 2019). The hydrographic centres of most of these rivers are not within Ogun State but in other states. Most of the perennial rivers often have braided channels and extensive flood plains and basins in lower parts. Majority of the subsequent and obsequent rivers and streams often dry up completely during the dry season while the consequent rivers often have their water levels and discharges reduced, thereby leaving extensive flood plains at their sides. The river valleys are the narrowest landform in the area. The river is a sluggish perennial stream in dry season but a turbulent one during the wet season. This relief can be described as undulating and the drainage is dendritic (Ishola, 2019).

Physiography and Geology of the Study Area

The physiography of the study area is that of extensive lowland that is generally undulating with a gently sloping dissected escarpment known as southern uplands as reported by Jones and Hockey (Ishola *et al.,* 2021). The area is drained mainly by Ewekoro River which according to (Ishola *et al.,* 2021) is obsequent, endorcic and forms a dense network all over the area with anstromatic pattern along its course. In terms of regional geology, the study area belongs to the eastern part of the Dahomey Basin extending from the Volta Delta (Southwestern Ghana) to the western flank of the Niger Delta in Nigeria (Ogbe, 1972). The stratigraphy of the basin has already been studied by various authors (Ishola *et al.,* 2021). However, the general succession of the sedimentary rock units of Ogun State which consists of Abeokuta formation lying directly above the basement complex is that of underlying rock which comprises of Abeokuta Group, followed by Ewekoro, Akinbo, Oshosun and Ilaro formations respectively while on top of Ilaro formation is the coastal plain sands (Benin formation) (Nton, 2006).

Overlying the Abeokuta Group conformably is the Imo group, which comprises of shale, limestone and marls. The two-lithostratigraphic units under this group are: Ewekoro formation and Akinbo formation. Adegoke (1977) described the formation as consisting of shaly limestone and is divided it into three microfacies. Ogbe (1972) further modified this and propose a fourth unit. The Ewekoro formation also overlies the Araromi formation in the eastern Dahomey basin being an extensive limestone body which is traceable over a distance of about 320Km from Ghana in the West, towards the eastern margin of the Dahomey basin in Nigeria. This type section is the limestone unit exposed in the Ewekoro quarry (Adegoke *et al.,* 1980) The Ewekoro Formation at the type locality Ewekoro is composed of about 11m – 12m of limestone. It is sandy at the base grading downward into Abeokuta formation. The Ewekoro Formation is overlain of Phosphatic Glauconitic grey shale (Ishola *et al.,* 2021). The limestone is classified (based on microfacies) into biomicrosparite, shelly biomicrites, algal biosparite and phosphatic biomicrites in that stratigraphic order. Elueze and Nton, (2004) has reported that the limestone is associated with shallow marine origin due to abundance of corraline, algae, gastropods, pelecypods, echinoid fragments and other skeletal debris. It is Paleocene in age. Overlying the Ewekoro formation is Akinbo formation and it comprises of shale, glauconitic rock bank, and gritty sand to pure grey and with little clay lenses of limestone sequence from Ewekoro formation grades literally into the Akinbo shale very close to the base (Ogbe, 1972). The claystones are concretionary and are predominantly kaolinite. The base is characterized by the presence of a glauconitic band with lenses of limestones (Ogbe, 1972; Nton, 2001). This unit is the lateral equivalent if the Imo formation in the southeastern Nigeria. Ogbe (1972) demonstrated that the shales on either side of Okitipupa Ridge differ markedly from each other in physical features. He then proposed the name Akinbo formation for the unit in the western side of the ridge, and selected the section exposed in the Ewekoro and Shagamu quarries as the type locality. The age of the formation is Paleocene to Eocene. Overlying the Akinbo formation in Imo group is the Oshosun formation. It is a sequence of mostly pale greenish-grey laminated phosphatic marls, light grey white-purple clay and shale with interbeds of sandstones. The shale is thickly laminated and glauconitic. It also consists of claystone underlain by argillaceous limestone of phosphatic and glauconitic materials in the lower part of the formation. According to Okosun (1998), the basal beds consist of the following facies; sandstones, mudstones, claystones, clay-shale or shale. This formation is phosphate-bearing deposits which are best developed near the Oshosun village by Russ in 1924 (Ishola *et al.,* 2021). Eocene age has been assigned to this formation (Agagu, 1985; Obaje, 2009). The sedimentation of the Oshosun formation was followed by a regression, which deposited the sandstone unit of Ilaro formation (Ishola and Gbadebo, 2024) conformably overlying the Oshosun formation and consists of gritty clay, gritty sand, massive and yellowish brown shale, poorly consolidated and cross-bedded sandstones, fine to coarse grained sand, bluish grained sand, bluish gray mudstones grading into glauconitic shale of the underlying Oshosun formation (Ishola and Gbadebo, 2024). The Benin formation is the youngest sedimentary unit in the eastern Dahomey Basin. This stratigraphic sequence is also known as coastal plain sands (Ishola *et al.,* 2021). It has a recent deposit called the tertiary alluvial deposit on it. It consists of soft, poorly sorted clayey sand and pebbly sands with lenses of clays and lignite. The sands are in parts cross-bedded and show transitional to continental characteristics. The age is from Oligocene to Recent. The thickness of the limestone is between 3m and 40m; the thickest being at Fashola community (38.3m) and the thinnest at Jaguna (1.6m). The range of overburden thickness is between 2m to 16m while the limestone thickness ranges between 1.5m to 38.2m. The reserve estimation was calculated to be 7.75 x 10^8 cubic meters and adjudged to be of economic value if exploited especially around Fashola town (Fidelis *et al.,* 2014).

MATERIALS AND METHODS

Theoretical Background

Electromagnetic method utilized the site response to the propagation of electromagnetic fields (Ishola *et al.,* 2023). Electromagnetic field comprised of an alternating electric intensity and magnetizing force. The speed at which EM can be made to propagate is much greater than the electrical method justifying the fact that electromagnetic method does not require contact with the ground. Therefore, an electromagnetic field can be developed by generating an alternating current through either a small coil comprising many turns of wire or a large loop of wire (Huang et al., 2022; Ishola *et al.,* 2023; Tyoh et al., 2025). The concept of electromagnetic field is better be defined in terms of four significant vector functions namely E, D, H and B,

where: E is the electrical field in V/m; D is the dielectric displacement in Coulomb/m²; H is the magnetic field intensity in A/m and B is the magnetic induction in Tesla (Ishola, 2019; Ishola *et al.*, 2023). Maxwell's equations adopting Faraday's law Experimental evidence reveals that all electromagnetic phenomena are subject to the following four Maxwell equations.

$\nabla E = -\frac{\partial B}{\partial t}-$ ....(1) (Ishola, 2019; Ishola *et al.,* 2023)

Faraday's law shows us how a time varying magnetic field produces an electrical voltage.

Maxwell's equations using Ampere's law

Ampere's law revealed how an electric current and/or a time varying electric field generate a magnetic field.

$\nabla H = J+\frac{\partial D}{\partial t}$ .... (2) (Ishola, 2019; Ishola *et al.,* 2023)

Maxwell's Equations infer that lines of magnetic induction are continuous and there are no presence not even a single magnetic poles.

div B = 0 .... (3) (Keary *et al.,* 2002; Ishola *et al.,* 2023)

It also infers that electrical fields can begin and end on electrical charges.

div D = q ....(4) (Keary *et al.,* 2002; Ishola *et al.,* 2023)

Subsidiary equations and wave equation

By applying the following subsidiary equations,

D = $\boldsymbol{\epsilon}$E, B = $\boldsymbol{\mu}$H, J = $\boldsymbol{\sigma}$E .... (5) (Keary *et* al., 2002; Ishola *et al.,* 2023)
where J = electrical current density in A/m^2 ; q = electric charge in Coulomb/m^3; ϵ = electrical permittivitiy; μ = magnetic permeability; σ = electrical conductivity (Ishola, 2019; Huang et al., 2022; Ishola *et al.,* 2023; Tyoh et al., 2025). From these four Maxwell equations the electromagnetic wave equation can hereby be derived.

Primary and Secondary Fields

There is no significant difference between the fields propagated above the surface and the ones penetrated through the subsurface (only slight reduction in amplitude is recorded). If a conductive anomalous body is present, alternating currents (Eddy currents) are induced within the conductor by the the magnetic component of the incident EM wave as displayed in Figure 5. The eddy currents generate their own secondary EM-field which travels to the receiver and the receiver equally detects the primary field which travels through the air (Ishola *et al.,* 2023). The resultant of the arrival of the primary and secondary field is authenticated and registered by the responds of the receiver (Ishola *et al.,* 2023). As a result of this field interaction, the measured response will differ both in phase and amplitude relative to the unmodulated primary field (Ishola, 2019; Ishola *et al.,* 2023). The detection of the presence of the encountered conductor as well as the necessary information on its geometry and electrical properties are revealed by these aforementioned differences between the transmitted and received electromagnetic fields. The depth of penetration of an electromagnetic field is dependent on the frequency as well as electrical conductivity of the medium through which propagation is made (Ishola *et al.,* 2023). Electromagnetic fields are therefore attenuated during their passage through the ground (GEONICS, 1990; Vogelsang, 1995; Ishola et al., 2021; Ishola *et al.,* 2023). The amplitude of EM-radiation serves as a function of depth relative to its original amplitude A_0 is given as

$A_d = A_0 e^{-1}$ ....(6) (GEONICS, 1990; Ishola, 2019; Ishola *et al.,* 2023)

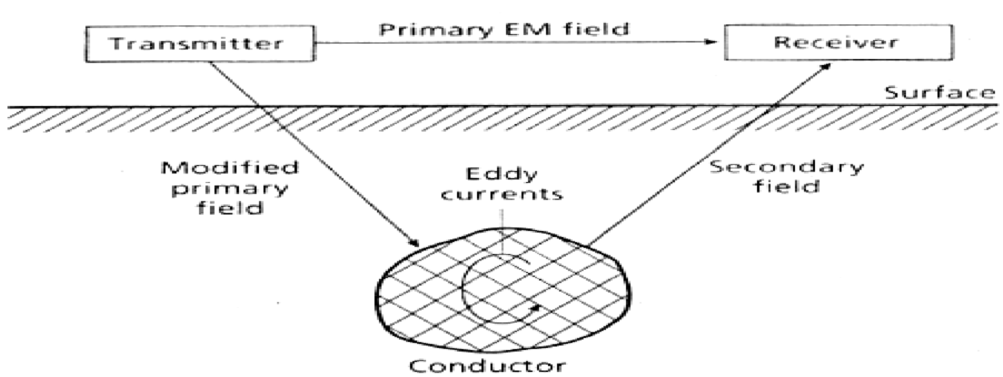

Figure 5: General Principle of Electromagnetic Surveying (Ishola *et al.,* 2023)

The depth at which the amplitude of the field A_d is decreased by the factor e^{-1} compared with its surface amplitude A_0 is defined as the depth of penetration d given as

$d = \frac{503.8}{\sqrt{\sigma f}}$ .... (7) (GEONICS, 1990; Ishola, 2019; Ishola *et al.,* 2023)

where d is in metres, the conductivity s of the ground is in Sm^{-1} and the frequency of the field is in Hz.

Just as both the frequency of the electromagnetic field and the conductivity of the ground decrease, the depth of penetration thus increases (Ishola *et al.,* 2023). Therefore, equation (7) represents a theoretical relationship. Whereby the frequency used as a result of the EM survey can be tuned to a desired depth range in any particular medium. Empirically, an effective depth of penetration z_e can be defined as the depth as the maximum depth at which a conductor may lie and still produce a considerable electromagnetic anomaly as shown in equation 8.

$z_e = \frac{10}{\sqrt{\sigma f}}$ .... (8) (GEONICS, 1990; Ishola, 2019; Ishola *et al.,* 2023)

Penetration is dependent on factors such as the nature and magnitude of the effects of near-surface variations in conductivity, the geometry of the subsurface conductor and instrumental noise making this relationship an approximate one. Constraints are placed on the EM method due to the dependence of the depth of penetration on frequency. Very low frequencies are normally difficult to develop and measure and the maximum penetration attainable in the field is usually of the order of 500m (McNeil, 1980b; Keary *et al.,* 2002; Omosuyi *et al.,* 2007; Ishola, 2019). 10m spacing are f = 10 Hz, d =503 m; f =100 Hz, d = 159 m and f = 1000 Hz, d = 50.3 m; are examples of different Depths of penetration and their corresponding frequencies**.**

Principle of Operation and Interpretation Technique of EM 34-3

The Electromagnetic Ground Conductivity Survey Method utilized in this work is based on a well established applied geophysical method. EM 34-3 terrain conductivity meter manufactured by Geonics Limited was obtained from the Department of Geosciences, University of Lagos, South-West Nigeria. A direct reading of the apparent conductivity (σa) of the ground in units of millimhos per metre (SI equivalent units are millisiemens per metre (mS/m) was provided by a change in conductivity of 5.0 mS/cm assumed to be measurable with the instrument. induction number has been defined as the ratio of the intercoil spacing

(s) divided by the skin depth (δ) (Ishola, 2019; Ishola *et al.,* 2021). In FDEM method, a GEONICS EM-34 meter possesses separate coils that were connected by a reference cable which provided the basis of the system in lengths of 10m, 20m and 40 m long. The effective depths of investigations are 7.5 m (HD) and 15 m (VD); for a frequency of 6.4 KHz and separation of 10 m; for a separation of 20 m and frequency of 1.6 Hz, is obtained a depth investigation of 15 m (HD) and 30 m (VD); for the separation of 40 m and frequency of 0.4 Hz, the investigation (GEONICS, 1990; Okpoli and Ozomoge, 2019; Ishola *et al.,* 2021; Huang et al., 2022; Ishola *et al.,* 2023; Tyoh et al., 2025).

The instrument operates on the measurements at Low Induction Number providing a direct reading of the quadrature as the apparent conductivity in mS/m. The secondary magnetic field is a complicated function of the inter-coil spacing, (s), the operating frequency (f), and the ground conductivity (σ). However, the technical definition is stated as "operation at low values of induction number" the very simple function of these variables in secondary magnetic field is incorporated in the design of the EM 34- 3 (Ishola, 2019; Ishola *et al.,* 2023). The product of s and the skin depth d, known as the induction number, is far less than unity. Therefore, the ratio of the intercoil spacing (s) divided by the skin depth is known as the induction number B where the induction number is less than one, then the ratio of the secondary to the primary of magnetic fields at the receiver is directly proportional to apparent conductivity. The ratio of the secondary (Hs) to primary (Hp) magnetic fields at the receiver at low induction n umbers (B<<1) is given by (Ishola, 2019; Okpoli and Ozomoge, 2019; Huang et al., 2022; Ishola *et al.,* 2023; Tyoh et al., 2025).

$$\frac{H_s}{H_p} = \frac{i\omega\ \mu\beta\sigma S^2}{4} \quad \text{...}(9)$$

Equation (9) provided the apparent conductivity as recorded by the instrument (Ishola *et al.,* 2023).

$$\sigma = \frac{i\omega\ \mu\beta\sigma S^2}{4}\left(\frac{H_S}{H_p}\right) \quad \text{...} \quad (10)$$

where: H_s is the amplitude of the secondary electromagnetic field at the receiver coil; H_p represents the amplitude of the primary electromagnetic field at the receiver coil; ω is the angular frequency (ω = $2\pi f$); f is frequency (Hertz); μB is the magnetic permeability of vaccum or free space (1.2566×10-6 m kg C^{-2}); σ represents the measured ground conductivity (mho/m); s is the inter coil spacing (m) while the presence of $i = \sqrt{-1}$ depicts that the quadrature component is measured (Ishola, 2019; Ishola *et al.,* 2023). Therefore, the ratio of H_s/H_p is proportional to the ground conductivity σ. Since depth d depends on the product of estimation of the maximum probable value of σ allows the selection of f such that the above condition of low induction number is satisfied. The depth of penetration is independent of the conductivity distribution of the subsurface but depends upon σ (Okafor and Mamah, 2012; Ishola *et al.,* 2023). Measurements taken at low induction number thus provide an apparent σ_a given by (McNeill, 1980b; Ishola, 2019; Ishola *et al.,* 2023).

$$\sigma_n = \frac{1}{\rho_a} = \left(\frac{4}{\omega\ \mu_0 S^2} \right) \left(\frac{H_S}{H_p} \right) q \quad \text{...(11)}$$

The above relationship enables the construction of elecromagnetic instruments that procures a direct reading of ground conductivity down to predetermined depth. The measuring system is also predesigned so as to ensure that with the selection of frequency f, for a given inter-coil separation (s), a designed response of Hp for a given transmitter, the only unknown Hs which is measured by the instrument with the subscript q denoting the quadrature phase (Ishola, 2019). Therefore, to measure the terrain conductivity in the field the search coil is either held horizontally (measurement in vertical dipole moment) or vertically (horizontal dipole mode). The results obtained from this field operations are generally displayed in the form of conductivity profiles. Today, inductive electromagnetic survey methods are widely harnessed to map near-surface geology by mapping variations in the electrical conductivity of the ground. These variations are generally functions of certain factors like changes in soil structure, clay content, porosity, resistivity of the soil water, and degree of water- saturation in the soil (GEONICS, 1990; Ishola, 2019; Ishola *et al.,* 2023).

Field Data Acquisition (Electomagnetic Ground Conductivity Survey)

In Papalanto study locations, five traverses were created with the station intervals of 500m. The length of each traverse ranged from 150m to 200m. Three traverses were established in the West and the East trending the North-South direction and two traverses to the North and South in the NW-SE direction. On each traverse, the first Profile was created in the W-E direction and second Profile created in the N-S direction with both Profiles having a Profile length of 200m. Electromagnetic profiles were selectively created in autonomous communities within Papalanto District for the primary purpose of outlining shallow conductive hydrogeological structures that could possibly be connected water circulation of the local hydrogelogic units of the area (Okafor and Mamah, 2012; Ishola *et al.,* 2023). The outcome of this investigation would be highly significant in in the future delimitation of a protected zone from contaminant infiltration (Ishola *et al.,* 2021). The investigated area has been a natural environment engaged with industrial operations in cement production, loading and transportation of cements and marketing of cement products; agricultural activities in sugarcane farming and food crops, artisanal works and numerous business activities. The myriads of these activities have led to the increase in human and biological population which in turn increase the demands for more water supplies and has consequently necessitated the need for preliminary investigation to meet the current challenge. The data was acquired along 5 North-South profiles with 2 electromagnetic measurements made along each traverse. The lengths of each traverse varied between 150 m and 200 m to show conductivity changes with distance and depth for each location with an intercoil spacing of 10m, 20m, and 40 m. The distance between the beginnings of each measurement points to the beginning of another measurement point was 500 m. At each site two measurements were made using both horizontal and vertical dipole mode. The main conductivity contrasts, can now be interpreted roughly as the shallow expression of fractures within the sedimentary filling of the hydrogeological structure of the area (Macdonald et al., 2005; Ishola *et al.,* 2021; Mamah, 2012; Ishola *et al*., 2023).

The procedure of the field operation involves An AC electric current is applied to a transmitter coil, the transmitter Tx is energised with an alternating current at a specific frequency, audio frequencies (100 - 5000 Hz), depth is 30 m (HD) and 60 m (VD) (GEONICS, 1990). Usually three frequencies are used seeking for different investigation depths; this generates a primary electromagnetic (EM) field in the coil. The primary time varying magnetic field generated from the transmitter and arising from this effect induces small current in the subsurface which is assumed uniform. These currents generate a secondary magnetic field, (Hs) which is sensed or detected, together with the primary field, (Hp) by the receiver coil, in the form of total field (HT) (Ishola *et al.,* 2023)**;** both magnetic fields are sensed by the receiver coil and a reading of apparent conductivity is given. The value of apparent conductivity depends on many factors. These are porosity, conductivity of pore fluid, pore surface area, degree of saturation of subsurface sediments, temperature, and (when present) clay content; the transmitter and receiver, are located vertically upward with the axis of the coil being horizontal to the subsurface; in the second mode (vertical magnetic dipole mode, VDM) the coils were placed lying flat horizontally with axis of the coil being vertical to the subsurface. Profiles with 10m, 20m and 40m of separation between transmitter and receiver were performed, using 6.4 KHz, 1.6 KHz and 0.4 KHz respectively in order to probe at varying depth and resolution; In either of the modes, the transmitter operator stops at the measurement station, the receiver operator (the researcher) then moves the receiver coil backwards or forwards until the meter indicates correct inter-coil spacing. At this point the receiver operator reads the terrain conductivity from a second meter. The procedure takes about 10 - 20 seconds. The measurement is first carried out in the horizontal coil orientation (vertical dipole mode) and later the corresponding vertical coil orientation (horizontal dipole mode) along the same profile. The vertical coil orientation gives information about the shallow subsurface while the horizontal coil orientation penetrates deeper into the subsurface (Ishola *et al.,* 2023); the apparent conductivity readings were taken at each station along the traverses and recorded in mmho/m (milli mho per metre) while other features and artifacts that could alter or affect the reading such as metals, vehicles and so on were noted against the station.

Data Processing and Interpretation

The acquired data were qualitatively checked by observing if negative apparent conductivity was recorded. Field note was used particularly as a guide to identify if certain anomalously high apparent conductivity values due to artifacts were present. The precautionary measures taken in the field among others using EM-34 transverses were restricted to areas far away from the overhead and underground utility cables and buried iron pipelines (Macdonald et al., 2005; Okafor and Mamah, 2012; Ishola *et al.,* 2023). The apparent conductivity reading of the horizontal dipole orientation on each traverse was plotted against station midpoint. This was also carried out separately for the vertical dipole orientation. The crossplots of apparent conductivity on the different spacing enabled a view of how the conductivity varies with depth. Qualitative analysis and interpretation were further carried out on the plotted data.

RESULTS AND DISCUSSIONS

Electromagnetic Profiling Survey Results of Ewekoro

The electromagnetic profiling data are presented as plots of conductivity (in mmho/m) against station intervals (in m). Typical EM profiles from the study area are shown in Figure 7 to Figure 16 while the characteristics of the true conductivity are displayed in Table 1.0. The Apparent Conductivity Profiles (EMPAP1 to

EMPAP2) along the traverses conducted in the West and across the NW-SE direction of Papalanto study area at 10m, 20m and 40m are displayed in Figure 7 and 8. The traverse displays appreciable variation in conductivity while locations of few recognizable positive peaks and broad anomalies which could be as a result of weathering of the subsurface geological horizon were delineated. These locations could be inferred as zones of interest for groundwater exploitation and consequently described as weathered to highly weathered/fractured zones and may serve as suitable aquiferous regions for water supply needs of the study area (MacDonald *et al.,* 2005). The observed varying degrees of conductivity values were delineated as represented in the plots with the most conductive area and the corresponding least conductive area respectively inferred to be conductive and resistive zones. The calculated true conductivity values for the first and second layer with their corresponding depth values were recorded for both horizontal and vertical dipole orientations in all the traverses. The highest true conductivity value of 1141.92 mS/m was recorded by Horizontal Dipole in the 2nd layer for EMPAP5 while the lowest true conductivity value of 78.9 mS/m was recorded by Vertical Dipole in the 1st layer for EMPAP6 (Figure 11 and 12).

The EM anomalies vary significantly; some are sharp while others are broad (Omosuyi *et al*., 2008). The traverse displays appreciable variation in conductivity while the areas where there are few recognizable positive peaks and broad anomalies were delineated against their conductivity values. Zones with peak positive vertical dipole anomalies are inferred conductive (fractured zones) typical of water–filled fissures (Alvin *et al.,* 1997), or effect of appreciable weathering (Ishola *et al.,* 2023). The higher the peak the deeper the rock fractured (Ugwu and Nwosu, 2009). These zones are considered priority areas for depth sounding. These locations could be inferred as zones of interests in groundwater exploitation and consequently described as weathered to highly weathered/fractured zones which may serve as suitable aquiferous regions for water supply needs of the study area (MacDonald *et al.,* 2005). In this traverse, locations of fewer or no observable linear spread and few haphazard variations were observed signifying the inhomogeneities of the study area despite the slight insignificant correlation between the horizontal and vertical dipole orientations. This is typically seen in EMPAP7, EMPAP8 and EMPAP10. The lowest and highest conductivity values of 86.29 and 1141.92 mmho/m were respectively recorded for both the vertical dipole and horizontal dipole moments (Figure 13, 14 and 16). The traverse displays significant variation in conductivity except at a distance of about 10m to 50m and 50m to 100m in Profile

EMPAP7 and 10m to 70m and 100m to 200m in Profile EMPAP8 where there are few observable positive peaks and broad anomalies of 205mmho/m, 198mmho/m, 179mmho/m, 199mmho/m, 172mmho/m and 190mmho/m. The observed varying degrees of conductivity values were delineated as represented in the plots with the most conductive area having a conductivity value of 205mmho/m and the least conductivity area having a conductivity value of 40mmho/m respectively inferred to be conductive and resistive zone. Consequently, Vertical Electric Sounding should be conducted in Profile EMPAP7 and EMPAP8. The traverse displays significant variation in conductivity except at a distance of about 10m to 90m in Profile EMPAP9 and 50m to 150m in Profile EMPAP10 where there are few observable positive peaks and broad anomalies of about 198mmho/m, 169mmho/m, 137mmho/m, 189mmho/m, 222mmho/m and 162mmho/m which could be as a result of the weathering of the subsurface geologic structures in the study locations. The observed varying degrees of conductivity values were delineated as represented in the plots with the most conductive area having a conductivity value of 222mmho/m and the least conductive area having a conductivity value of 45mmho/m respectively inferred as conductive and resistive zones; these are appreciable prospects for groundwater exploration. Consequently, other groundwater investigation techniques like Vertical Electric Sounding should be carried out in Profile EMPAP9 and EMPAP10. Varying high conductivity value range 64mmho/m to 198mmho/m, 45mmho/m to 169mmho/m and 45mmho/m to 137mmho/m were respectively recorded for 10m, 20m and 40m dipole spacing in a respective order obtained from the horizontal and vertical dipole orientations in the Electromagnetic Profiling of EMPAP9 while a conductivity range of values of 68 mmho/m to189mmho/m, 55mmho/m to 222mmho/m, 52mmho/m to 162mmho/m were equally recorded in increasing order of 10m, 20m and 40m dipole separations observed on the horizontal and vertical dipole orientations on the Electromagnetic Profiling of EMPAP10 in a respective order of varying investigation depth and resolution along the same traverse EMT_5. The high conductivity observed on both Profiles (EMPAP9 and EMPAP10) is indicative of probable invasions of the subsurface by the contaminant plumes; this contaminant plume is related to leachates from the exotic materials and decaying wastes from the surface percolating the subsurface through the porous and permeable layers of overlying rock thereby migrating its

Table 1.0: Characteristics of the True Conductivity in Papalanto

Papalanto EM Profiles	Delineated layers	True Conductivity HDM (mmho/m)	True Conductivity VDM (mmho/m)	Depth of Investigation (HDM) (m)	Depth of Investigation (VDM) (m)
EMPAP1	1st Layer	118	133.33	9	14
	2nd Layer	138	134.31	-	-
EMPAP2	1st Layer	122	116	4.3	14
	2nd Layer	127	121.88	-	-
EMPAP3	1st Layer	146	90	2	9.8
	2nd Layer	151.2	100	-	-
EMPAP4	1st Layer	150.59	86.29	7.8	11
	2nd Layer	158.92	91.11	-	-
EMPAP5	1st Layer	131.15	87.32	8.9	16
	2nd Layer	1141.92	94.55	-	-
EMPAP6	1st Layer	138	78.9	2	17
	2nd Layer	140.4	84.55	-	-
EMPAP7	1st Layer	167.48	96.78	7.8	9.2
	2nd Layer	176.34	98.18	-	-
EMPAP8	1st Layer	143.32	98.6	8.4	6.5
	2nd Layer	182.22	99.6	-	-
EMPAP9	1st Layer	121.13	106.92	3.1	10
	2nd Layer	123.99	121.96	-	-
EMPAP10	1st Layer	130	115.88	33	10.4
	2nd Layer	206	122.13	-	-

ways down to the subsurface. The results of the horizontal and vertical dipole orientations on both Profiles are strongly correlated with few sinusoidal peaks and haphazard variation with high amplitude peak points are suggesting heterogeneity of the subsurface area under investigation. The Profiles are suggestive of the subsurface being polluted to a reasonable level of influence of the contaminant seepages which may possibly degrade the groundwater quality of the investigated locations. The distribution of Papalanto subsurface conductivity Profiles and their corresponding conductivity variation in each profile are displayed in Figure 17 and 18 for the first layer and Figure 19 and 20 for the second layer.

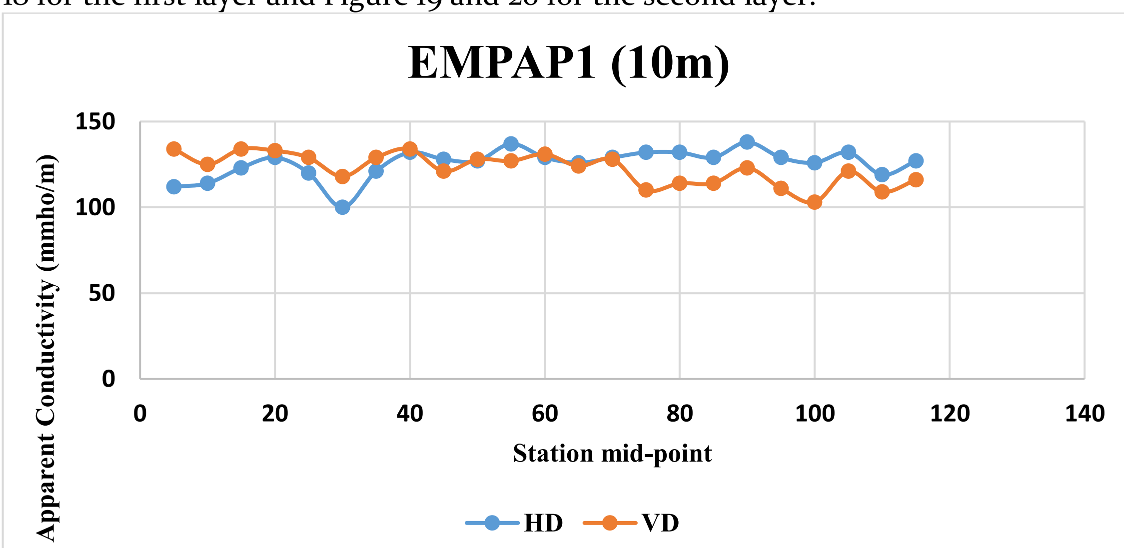

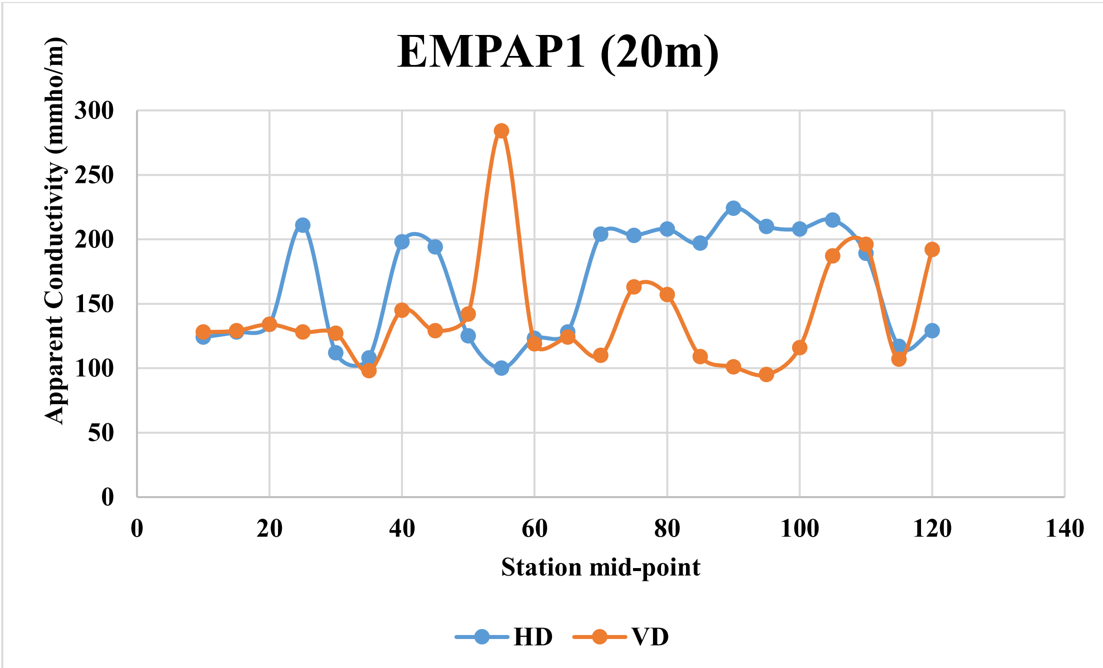

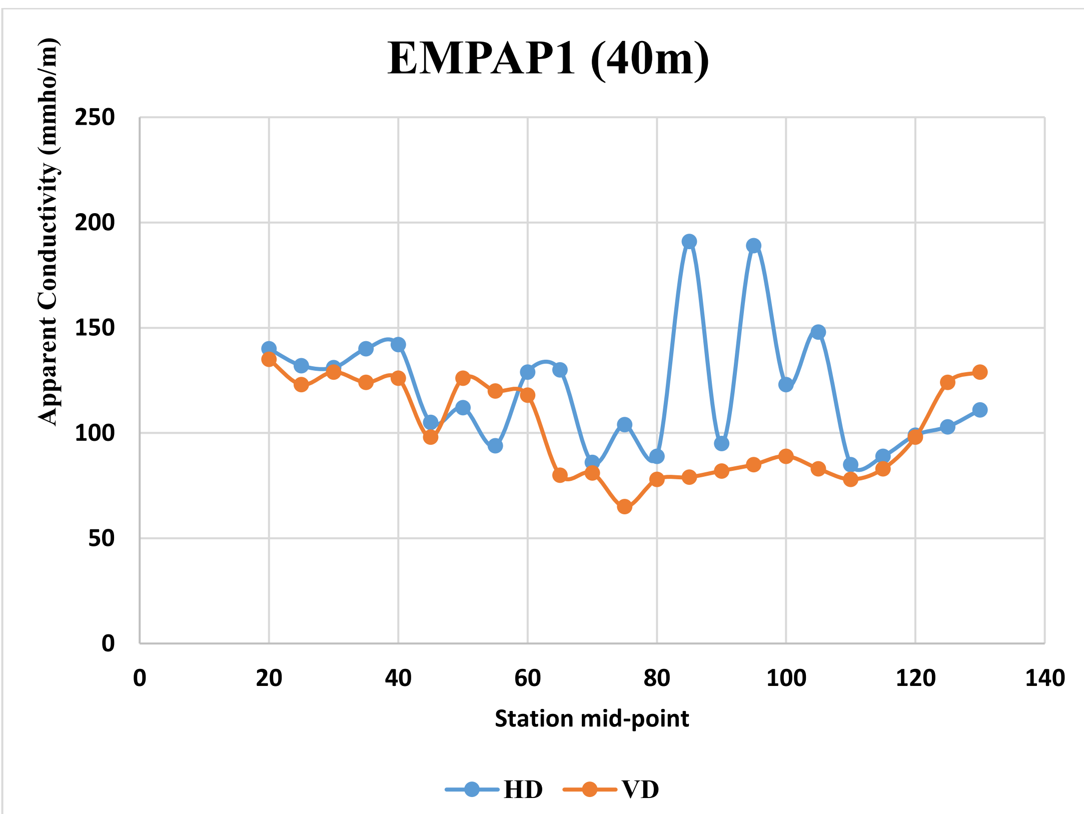

Figure 7: Plot and Values of Apparent and Real Conductivity of Horizontal Dipole Orientations along Papalanto Traverse 1 (Profile 1)

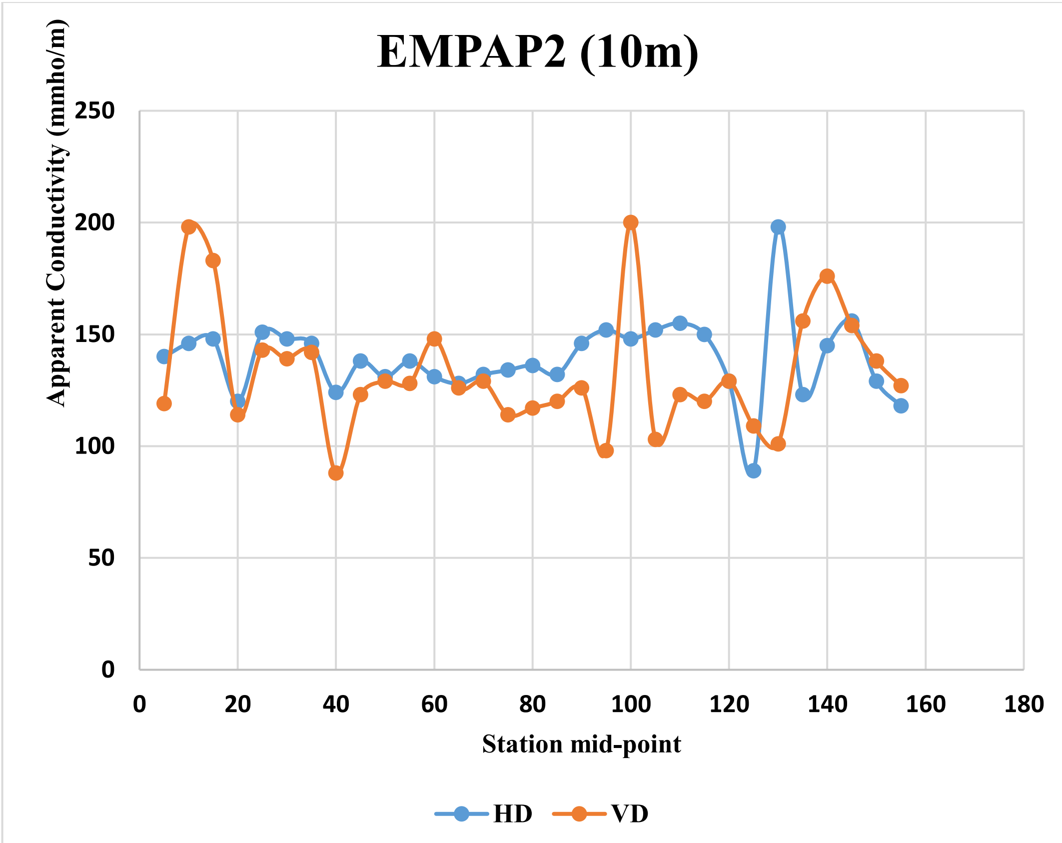
EMPAP2 (10m)
Apparent Conductivity (mmho/m)
250
200
150
100
50
0
0
20
40
60
80
100
120
140
160
180
Station mid-point
HD
VD

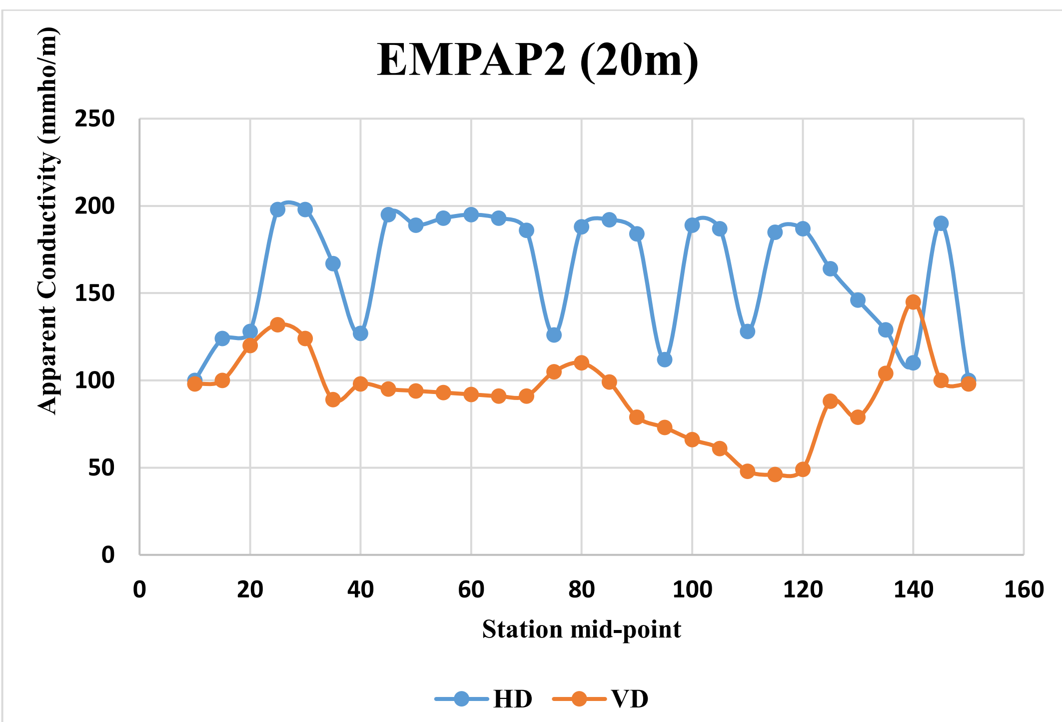
EMPAP2 (20m)
Apparent Conductivity (mmho/m)
250
200
150
100
50
0
0
20
40
60
80
100
120
140
160
Station mid-point
HD
VD

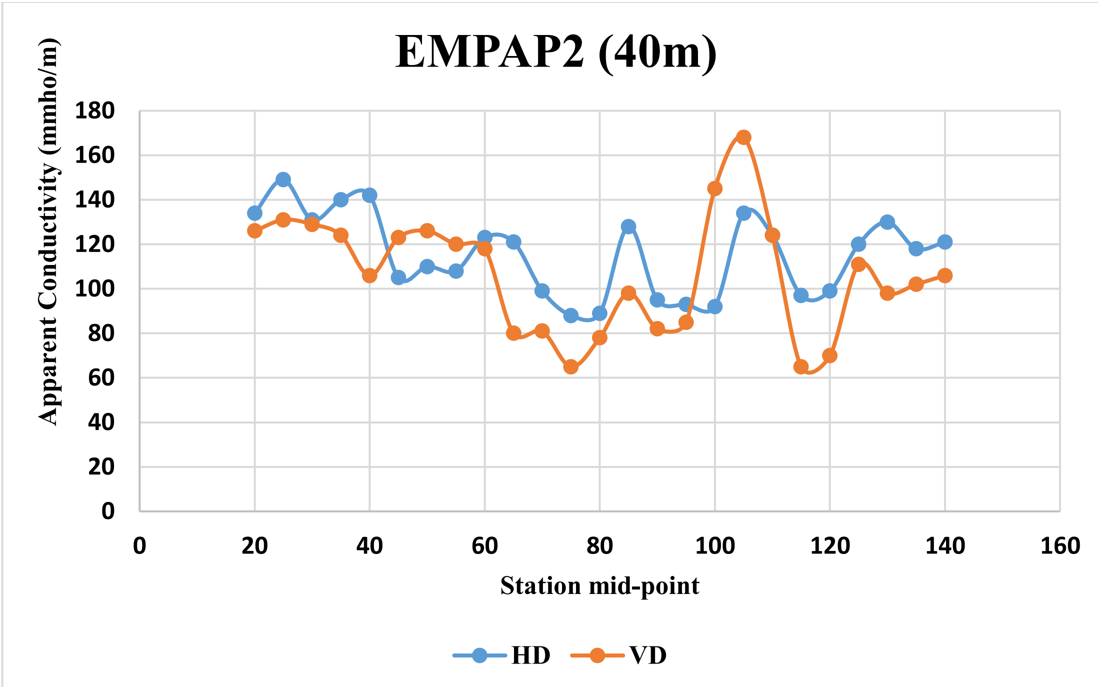

Figure 8: Plot and Values of Apparent and Real Conductivity of Horizontal Dipole Orientations along Papalanto Traverse 1 (Profile 2)

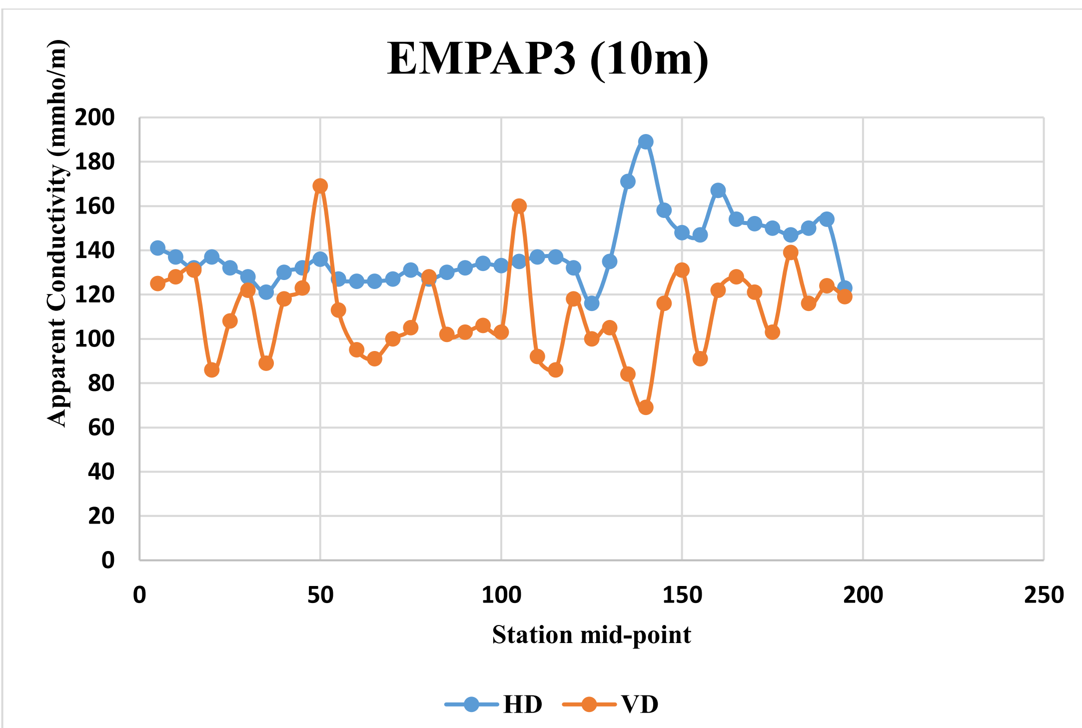

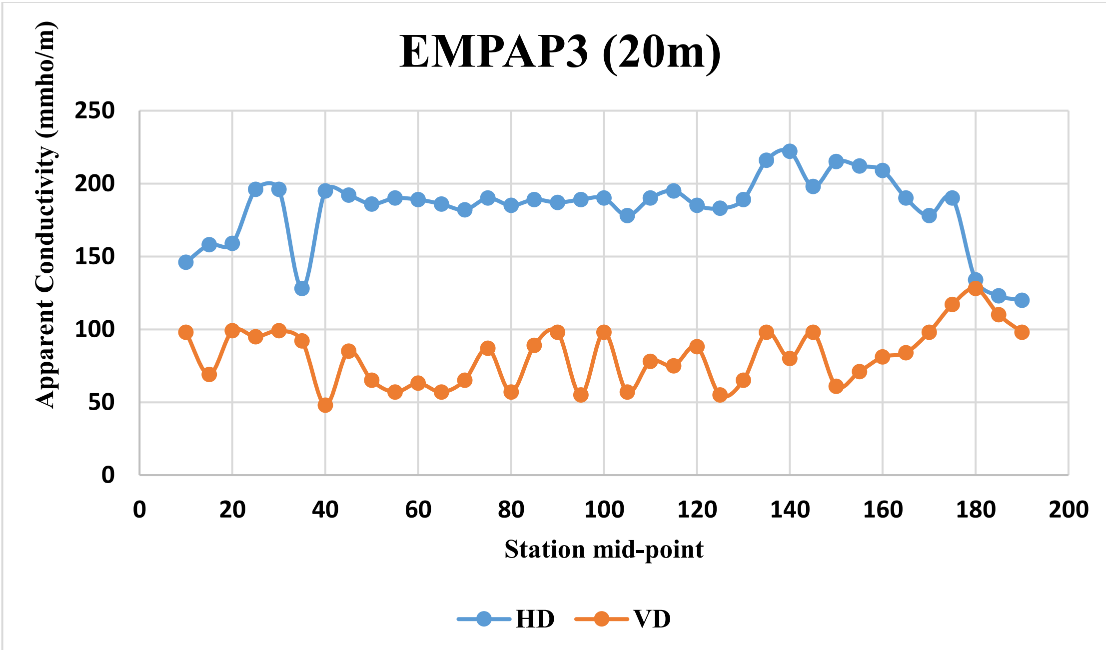

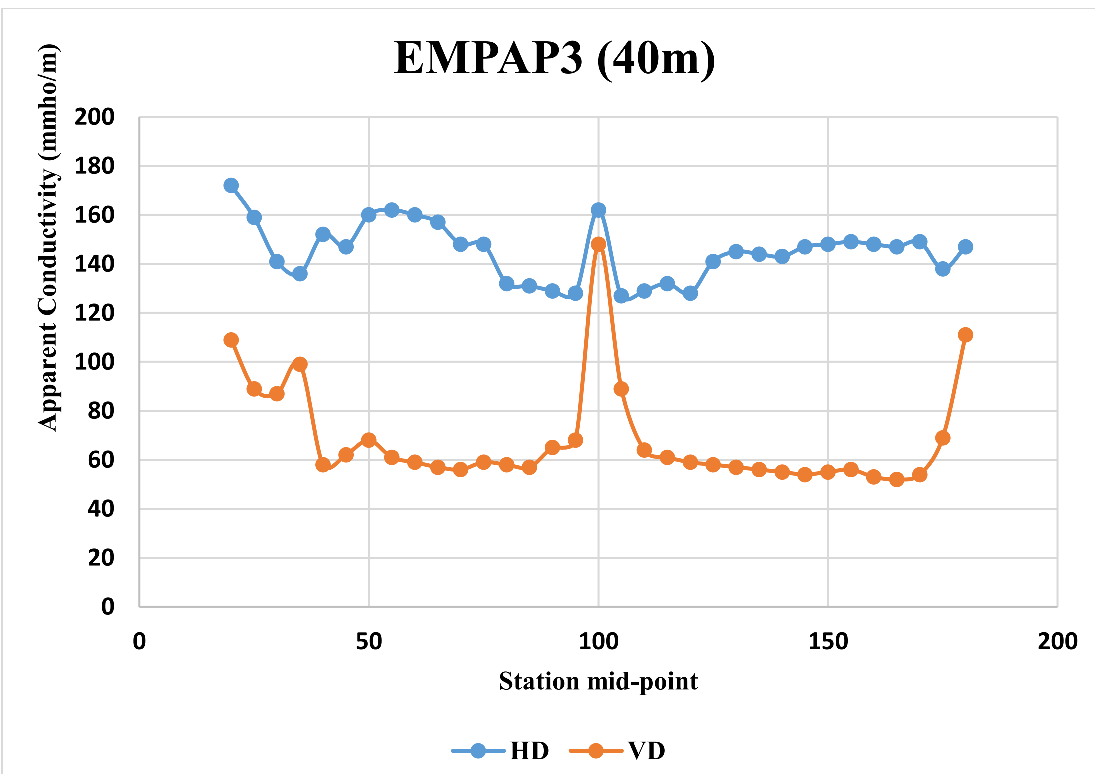

Figure 9: Plot and Values of Apparent and Real Conductivity of Horizontal Dipole Orientations along Papalanto Traverse 2 (Profile 3)

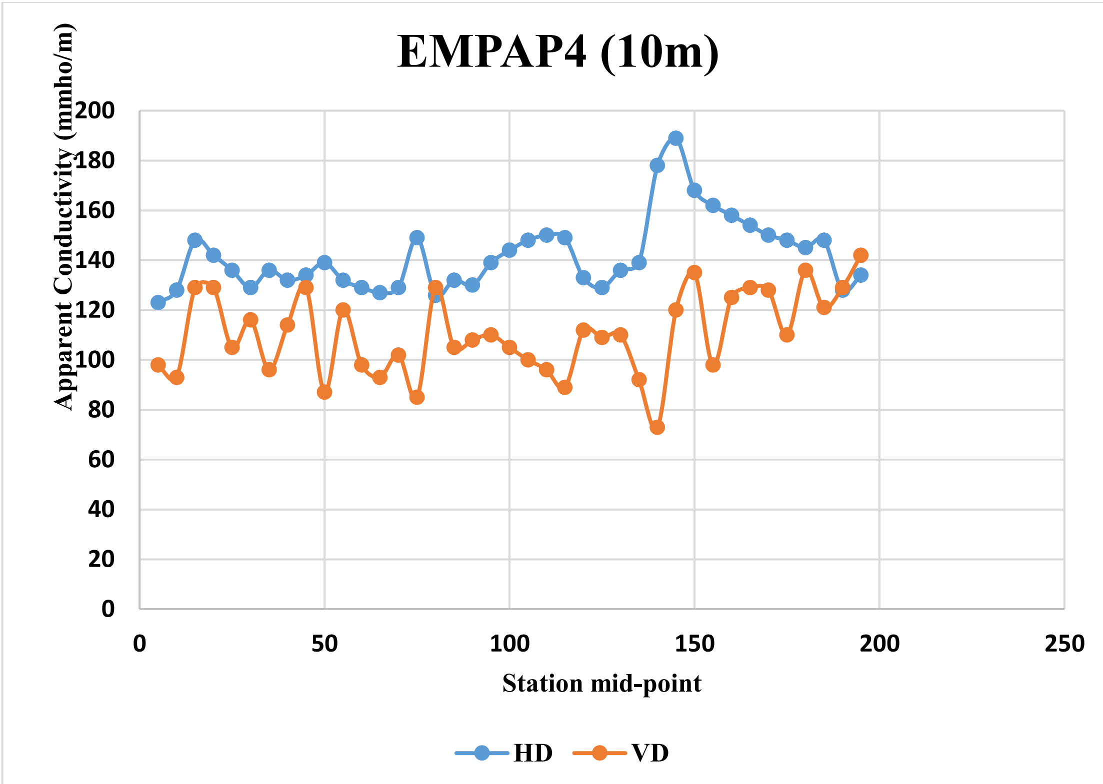
EMPAP4 (10m)
Apparent Conductivity (mmho/m)
0
20
40
60
80
100
120
140
160
180
200
0
50
100
150
200
250
Station mid-point
HD
VD

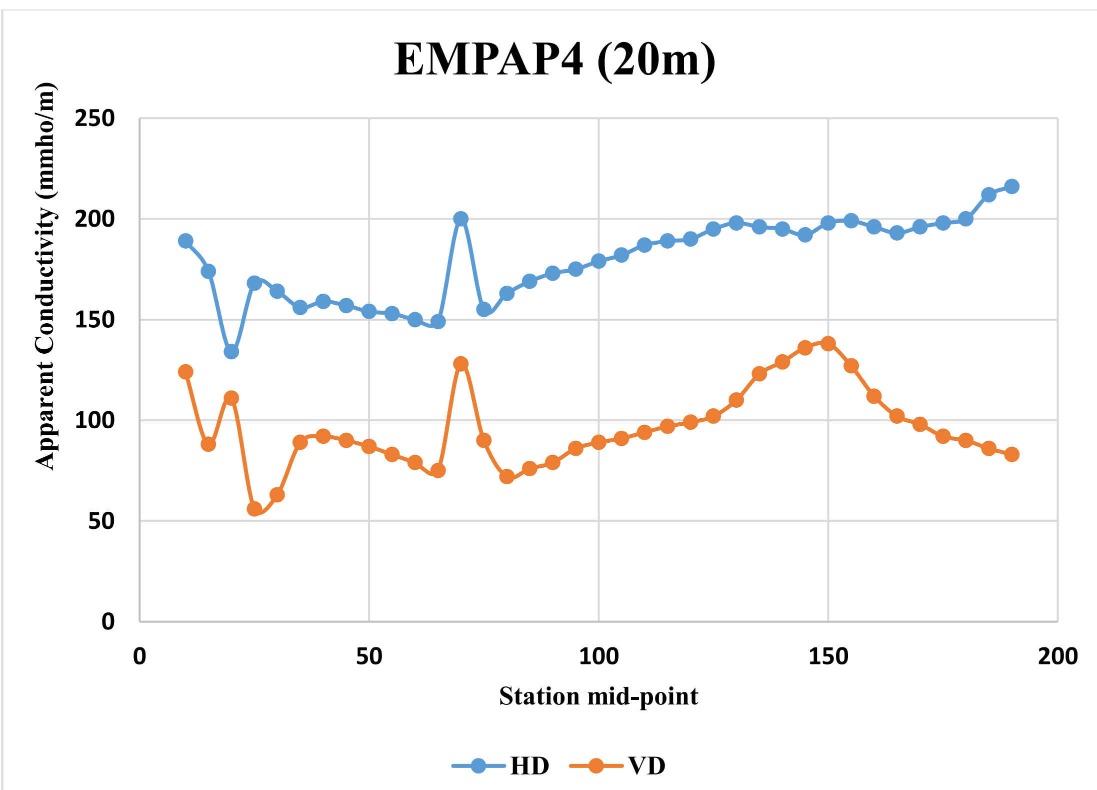
EMPAP4 (20m)
Apparent Conductivity (mmho/m)
0
50
100
150
200
250
0
50
100
150
200
Station mid-point
HD
VD

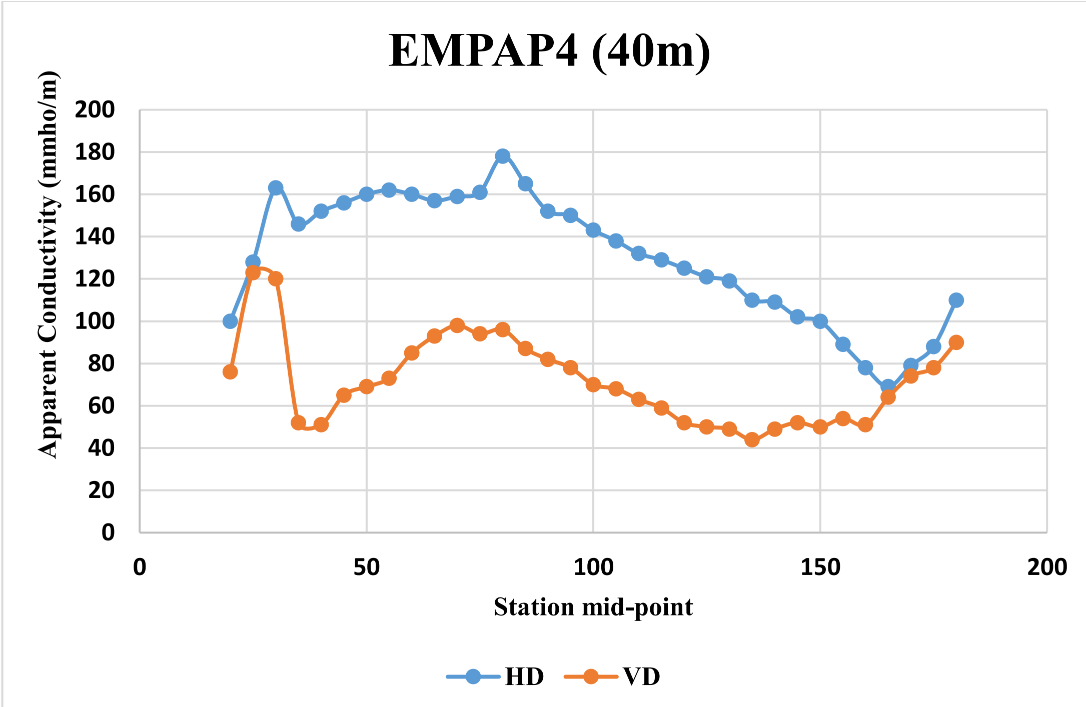

Figure 10: Plot and Values of Apparent and Real Conductivity of Horizontal Dipole Orientations along Papalanto Traverse 2 (Profile 4)

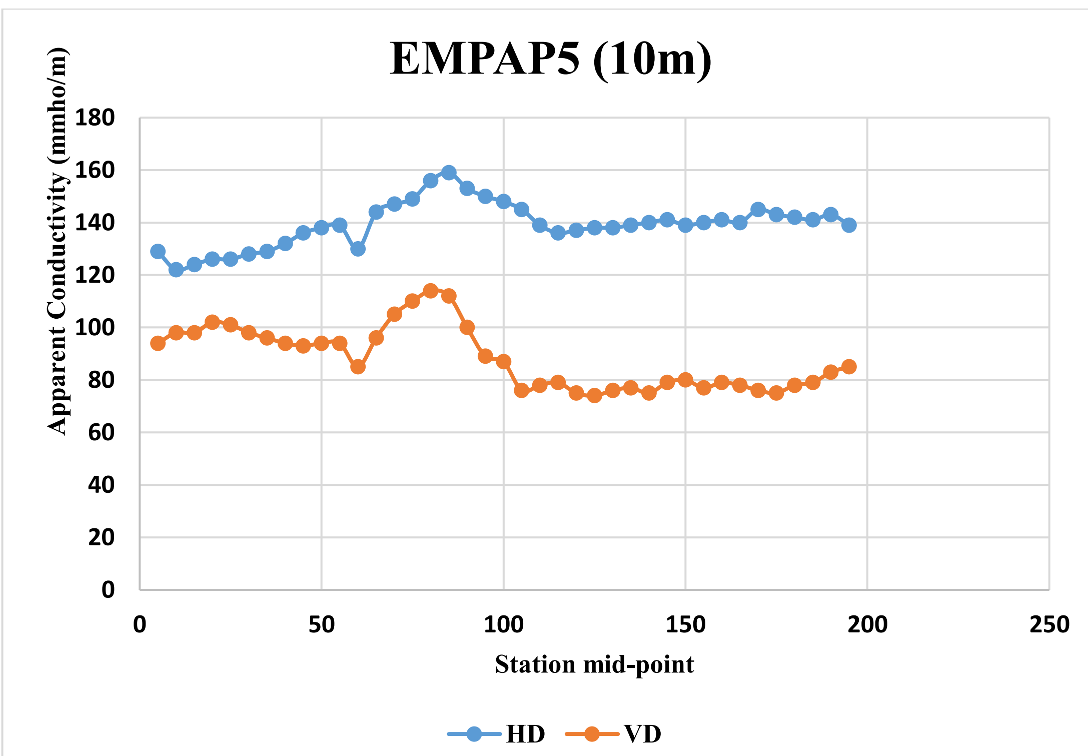

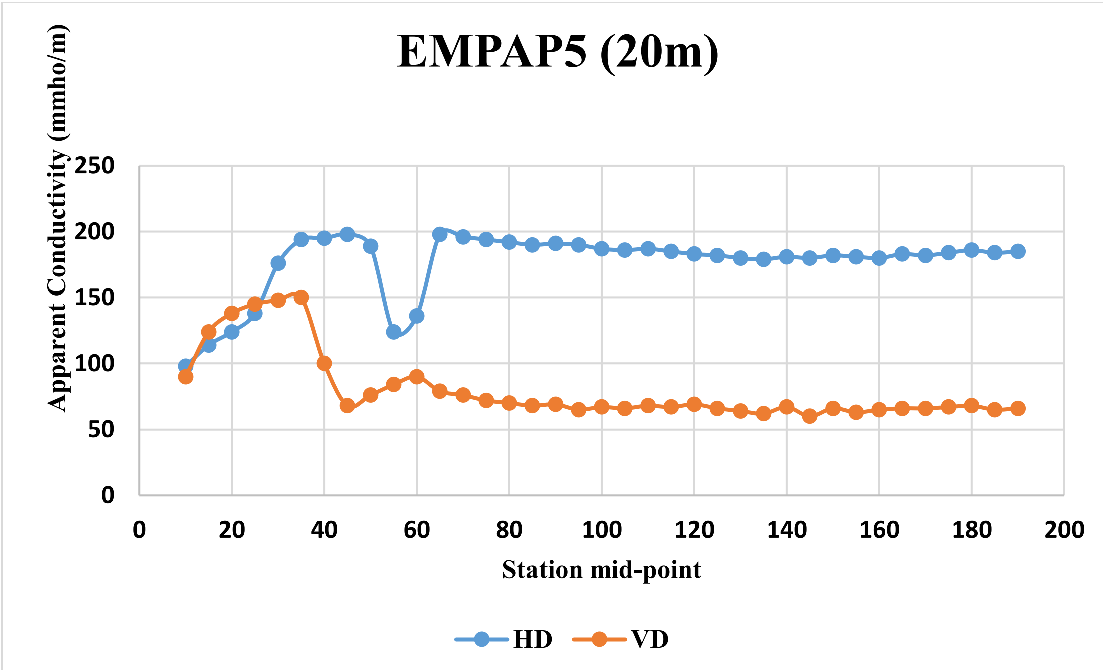

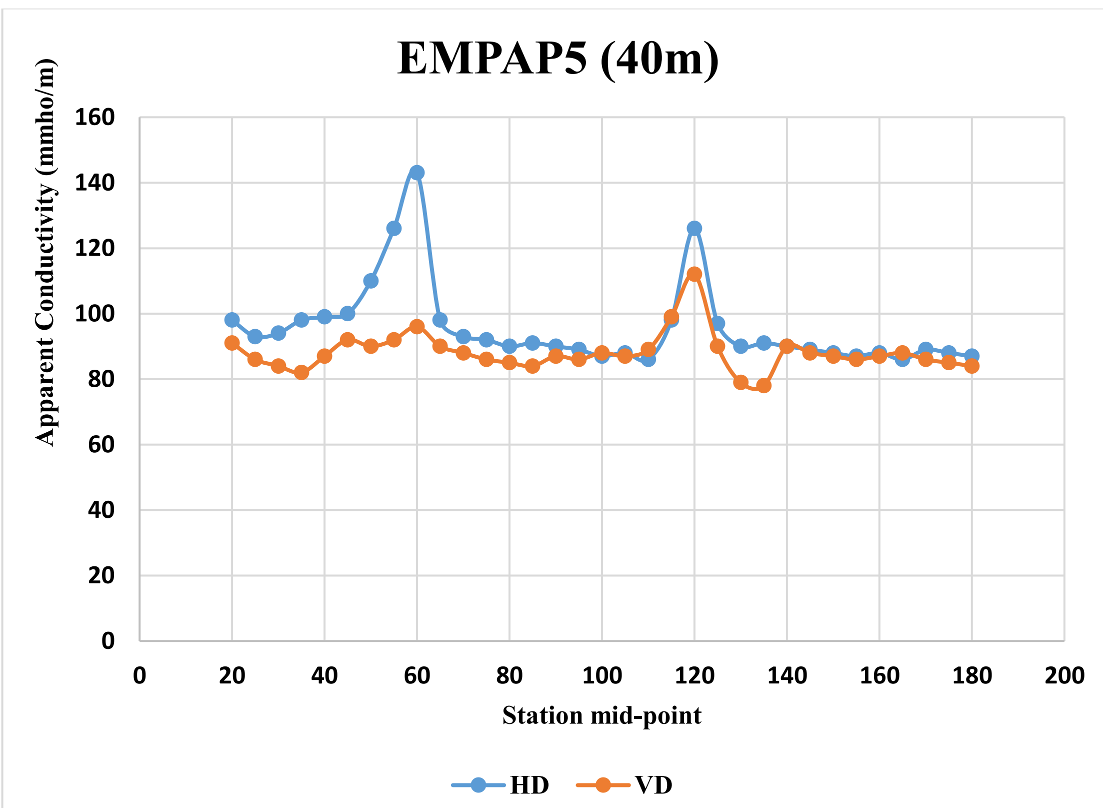

Figure 11: Plot and Values of Apparent and Real Conductivity of Horizontal Dipole Orientations along Papalanto Traverse 3 (Profile 5)

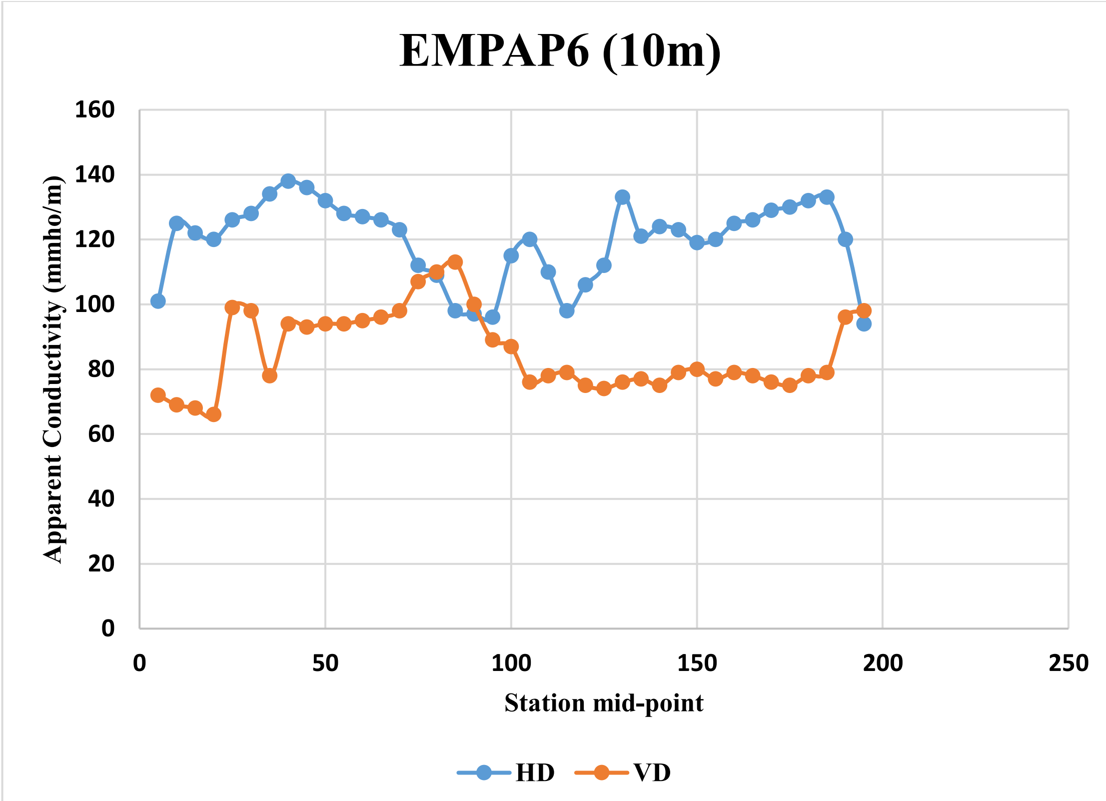
EMPAP6 (10m)
Apparent Conductivity (mmho/m)
0
20
40
60
80
100
120
140
160
0
50
100
150
200
250
Station mid-point
HD
VD

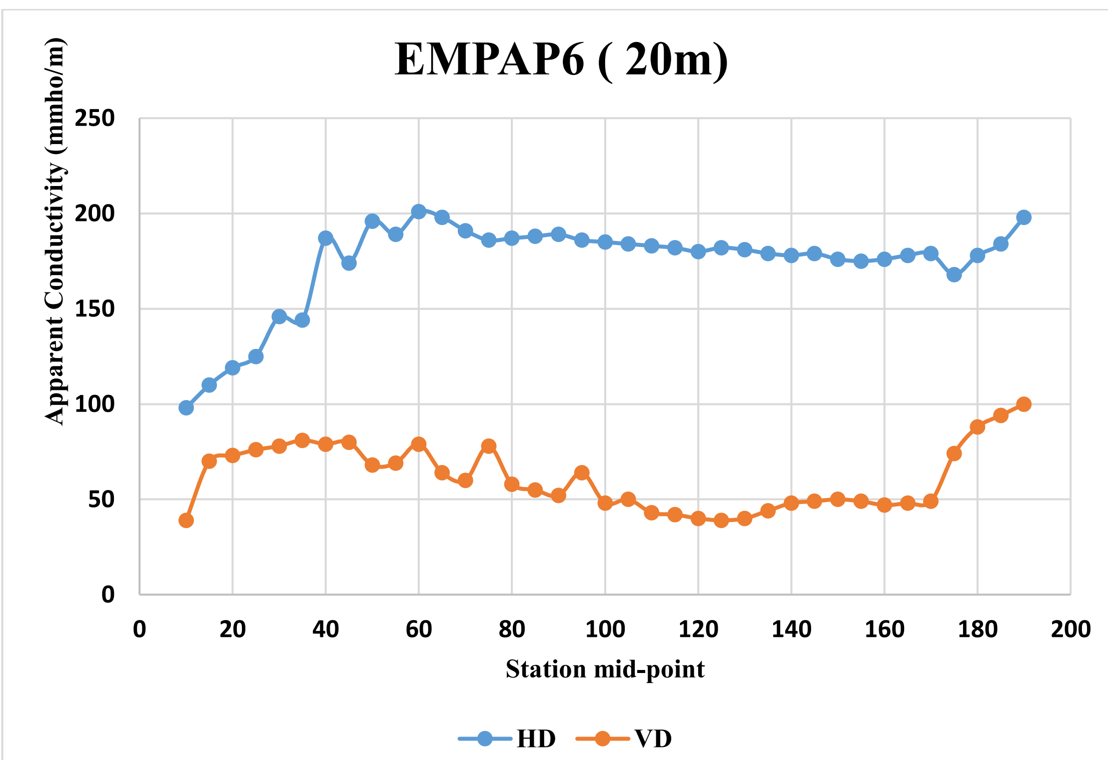
EMPAP6 (20m)
Apparent Conductivity (mmho/m)
0
50
100
150
200
250
0
20
40
60
80
100
120
140
160
180
200
Station mid-point
HD
VD

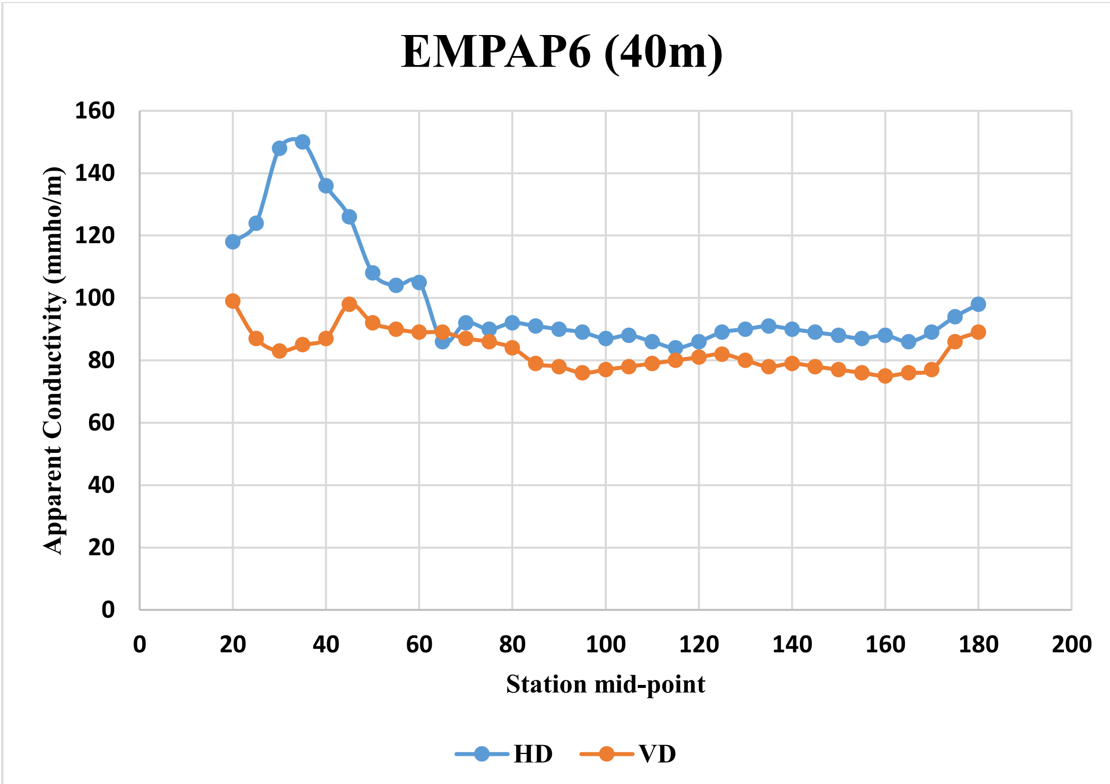

Figure 12: Plot and Values of Apparent and Real Conductivity of Horizontal Dipole Orientations along Papalanto Traverse 3 (Profile 6)

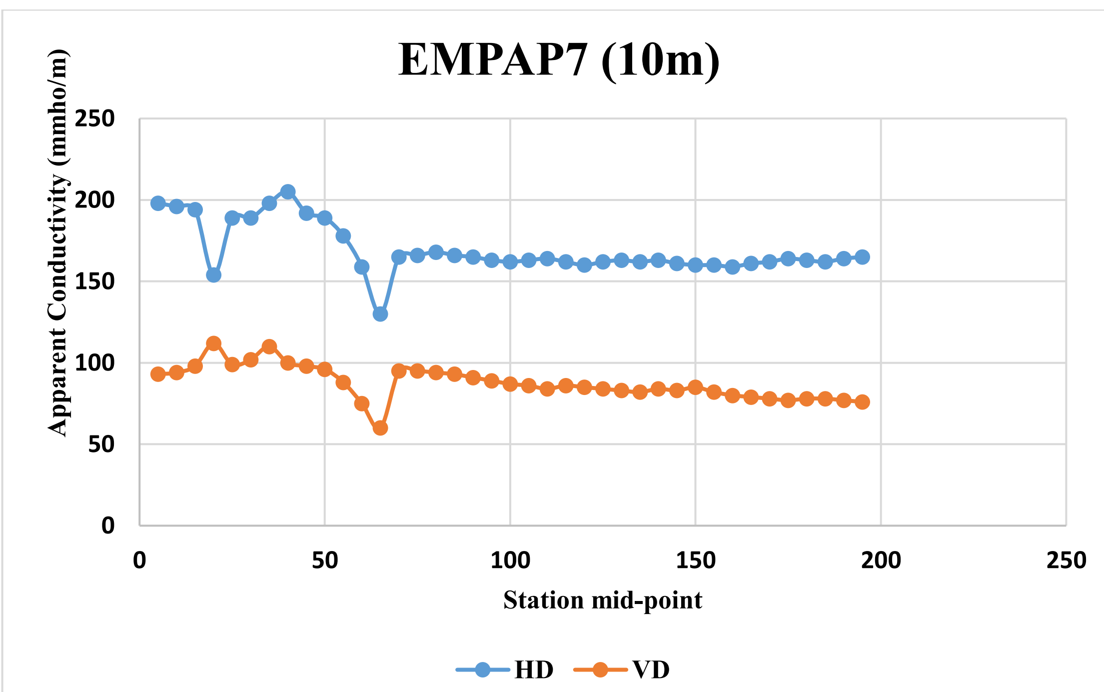

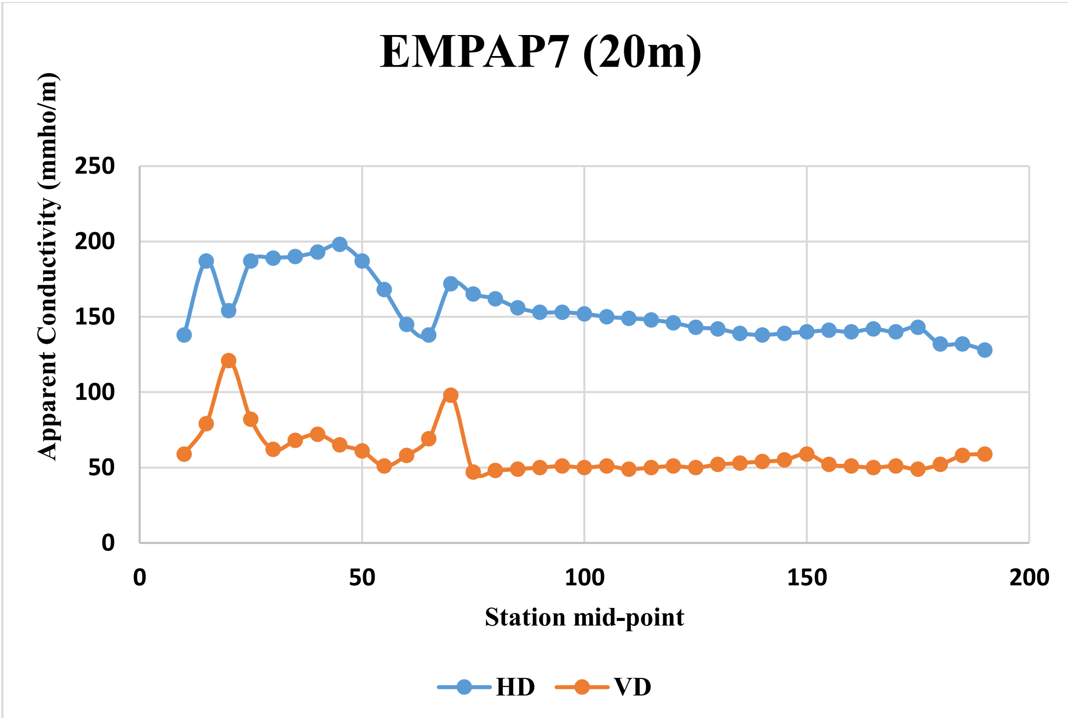

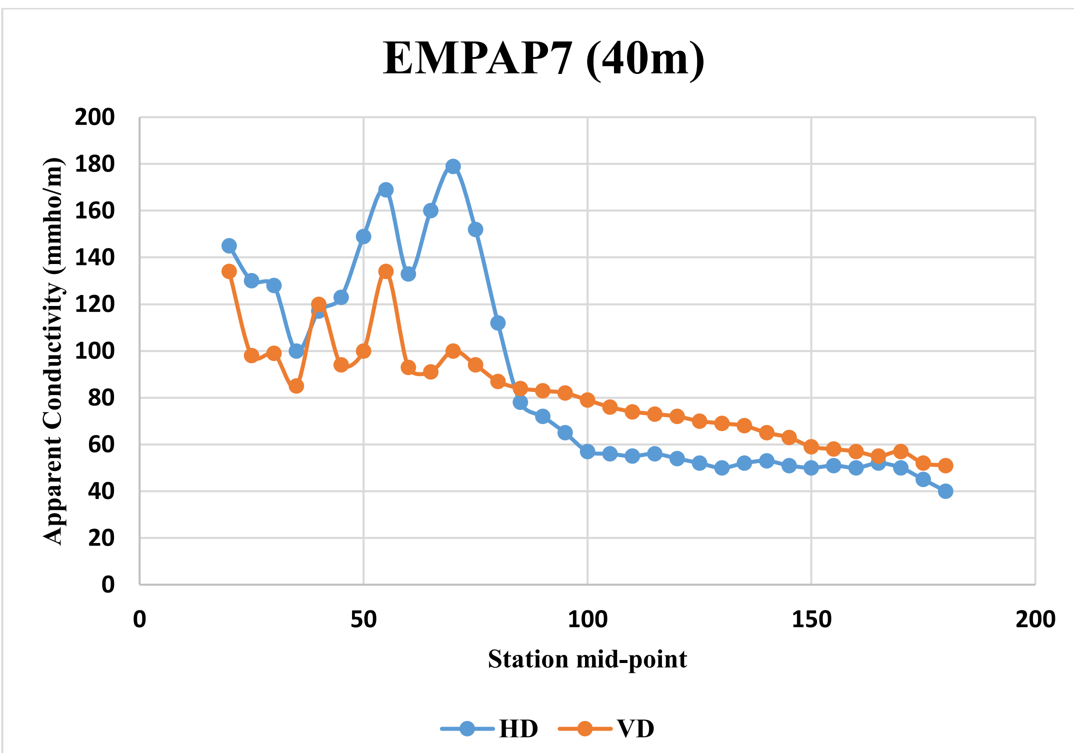

Figure 13: Plot and Values of Apparent and Real Conductivity of Horizontal Dipole Orientations along Papalanto Traverse 4 (Profile 7)

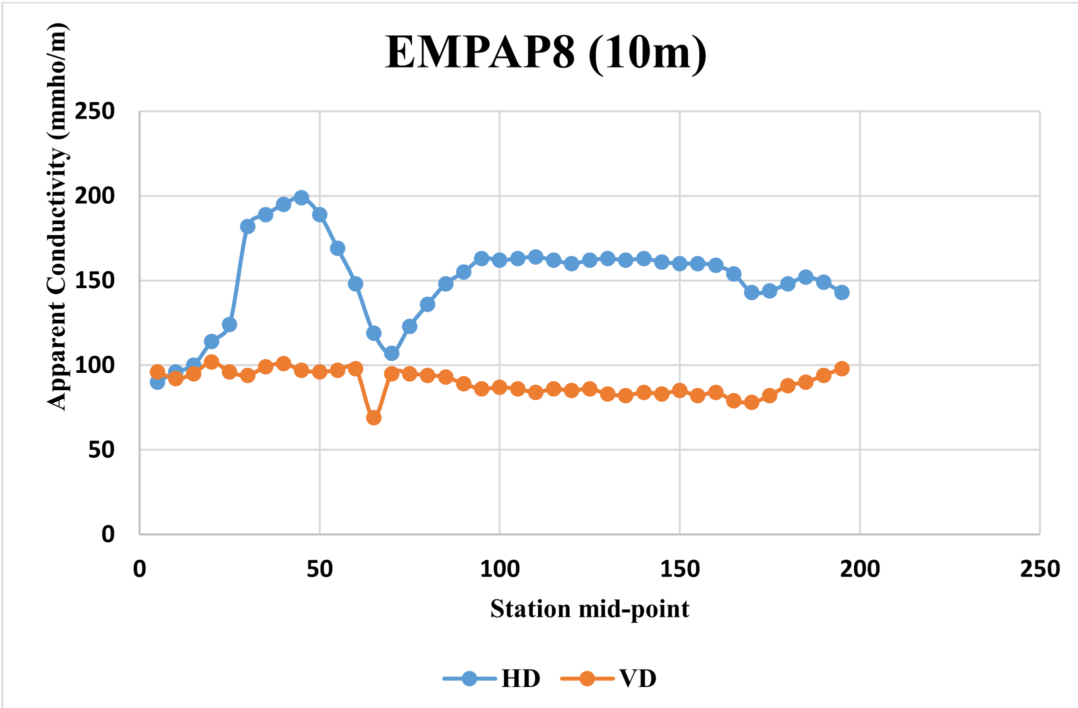
EMPAP8 (10m)
Apparent Conductivity (mmho/m)
250
200
150
100
50
0
0
50
100
150
200
250
Station mid-point
HD
VD

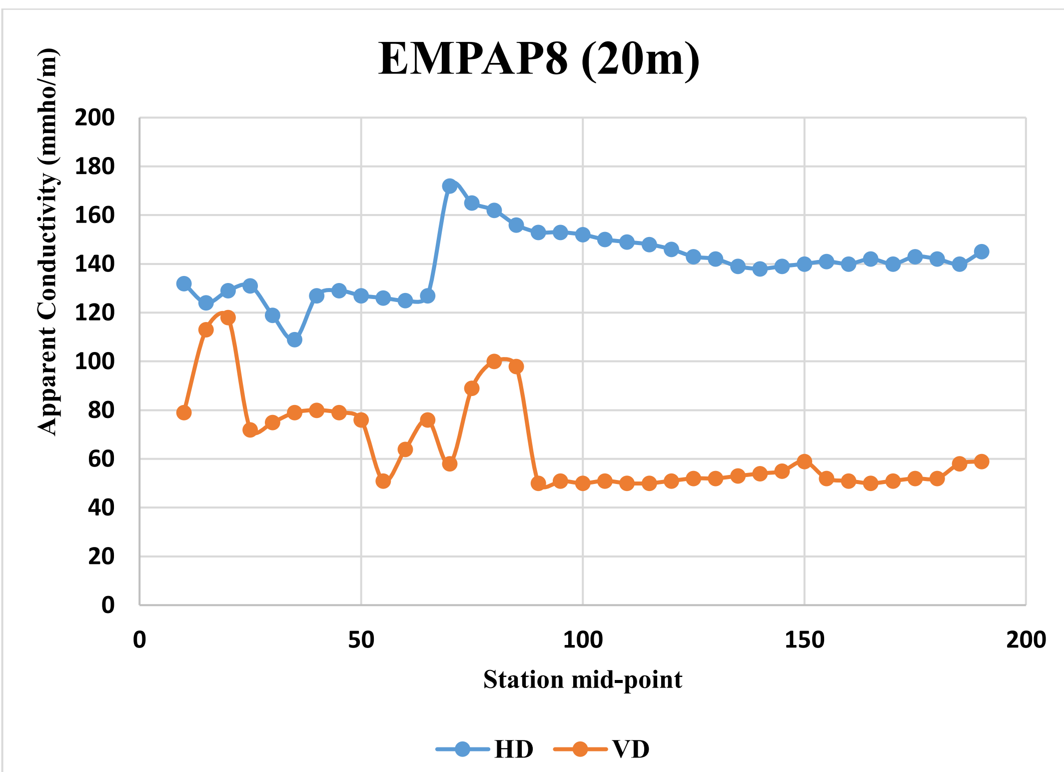
EMPAP8 (20m)
Apparent Conductivity (mmho/m)
200
180
160
140
120
100
80
60
40
20
0
0
50
100
150
200
Station mid-point
HD
VD

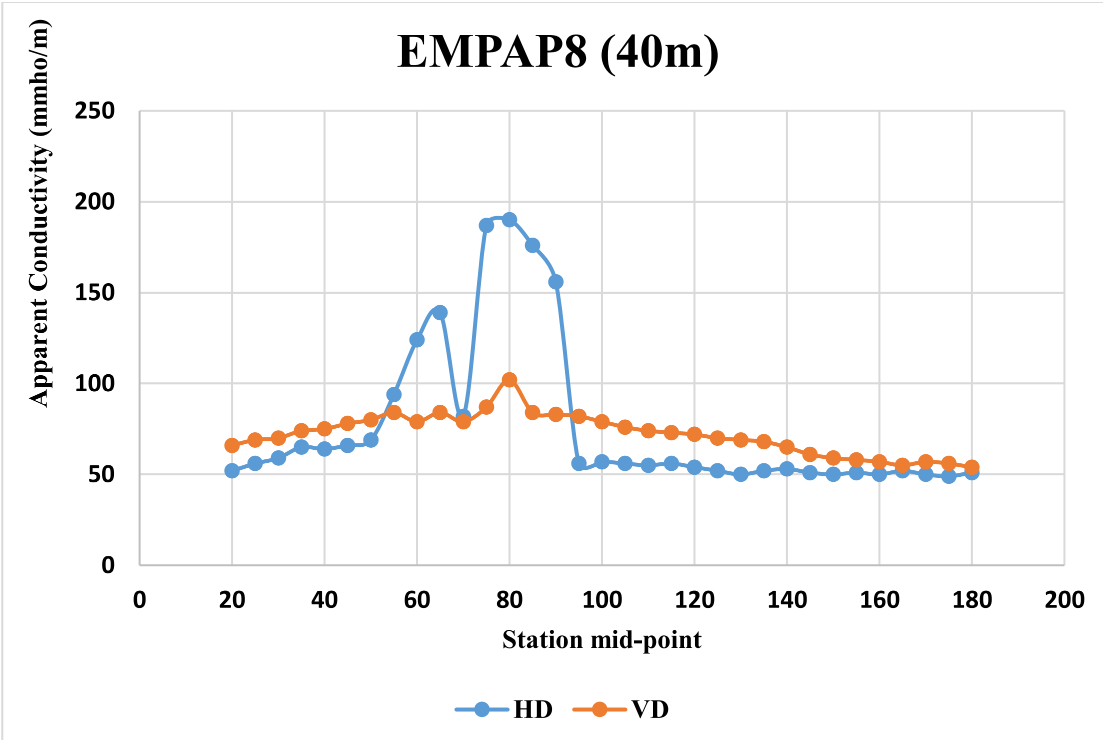

Figure 14: Plot and Values of Apparent and Real Conductivity of Horizontal Dipole Orientations along Papalanto Traverse 4 (Profile 8)

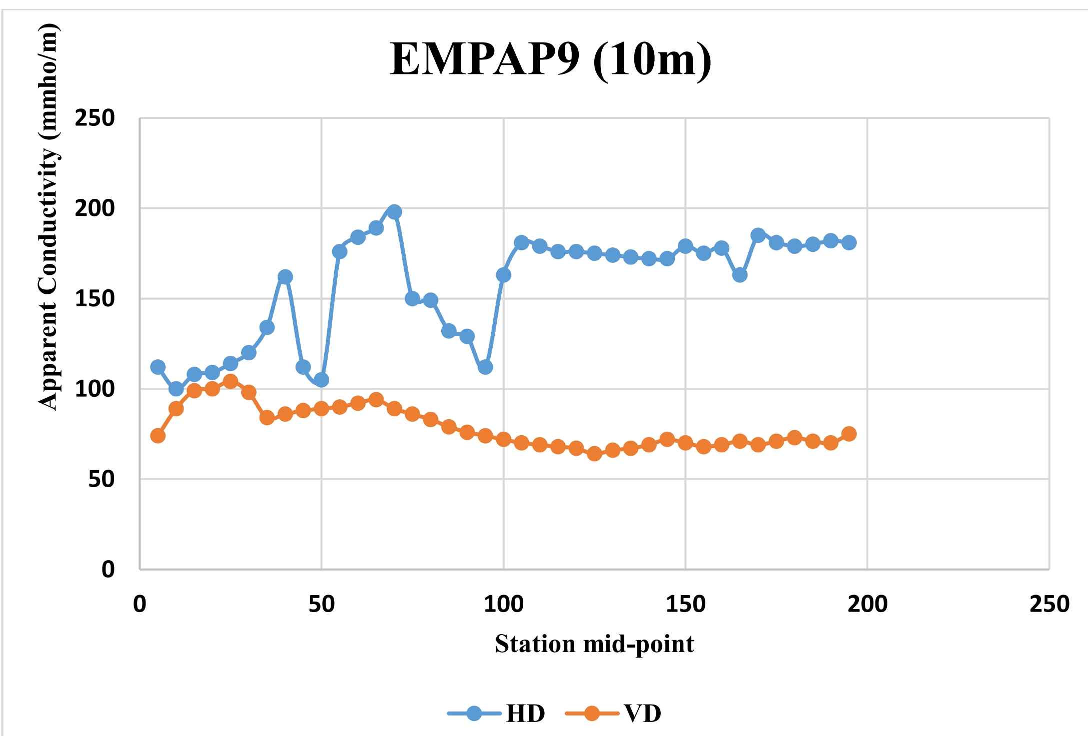

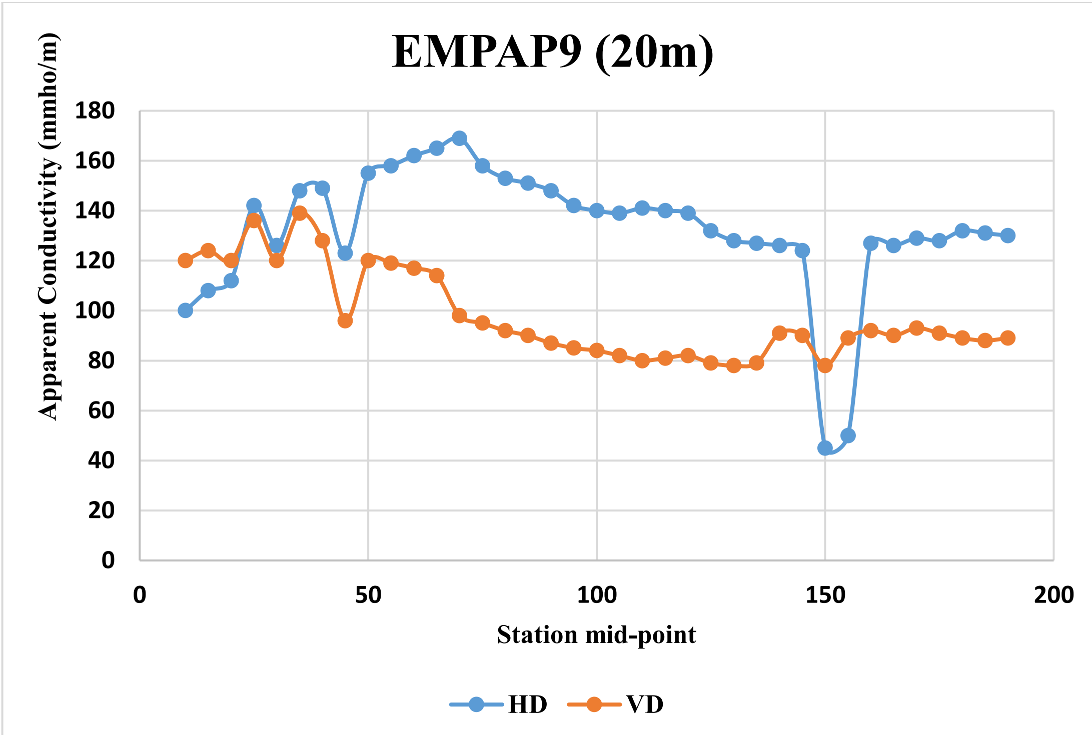

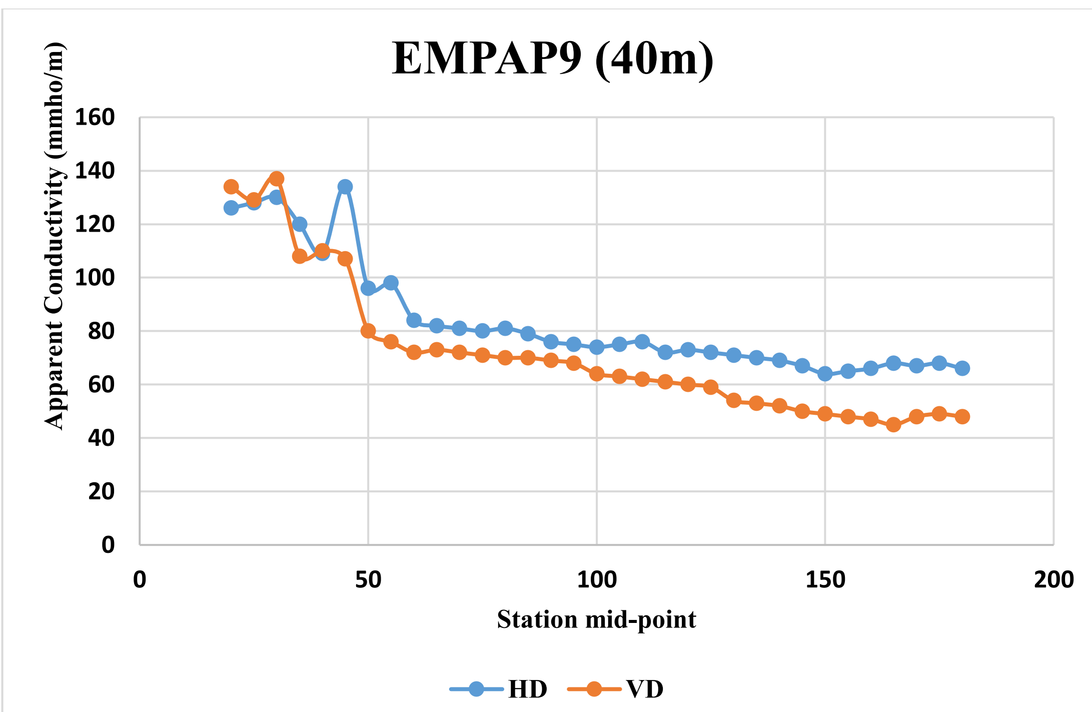

Figure 15: Plot and Values of Apparent and Real Conductivity of Horizontal Dipole Orientations along Papalanto Traverse 5 (Profile 9)

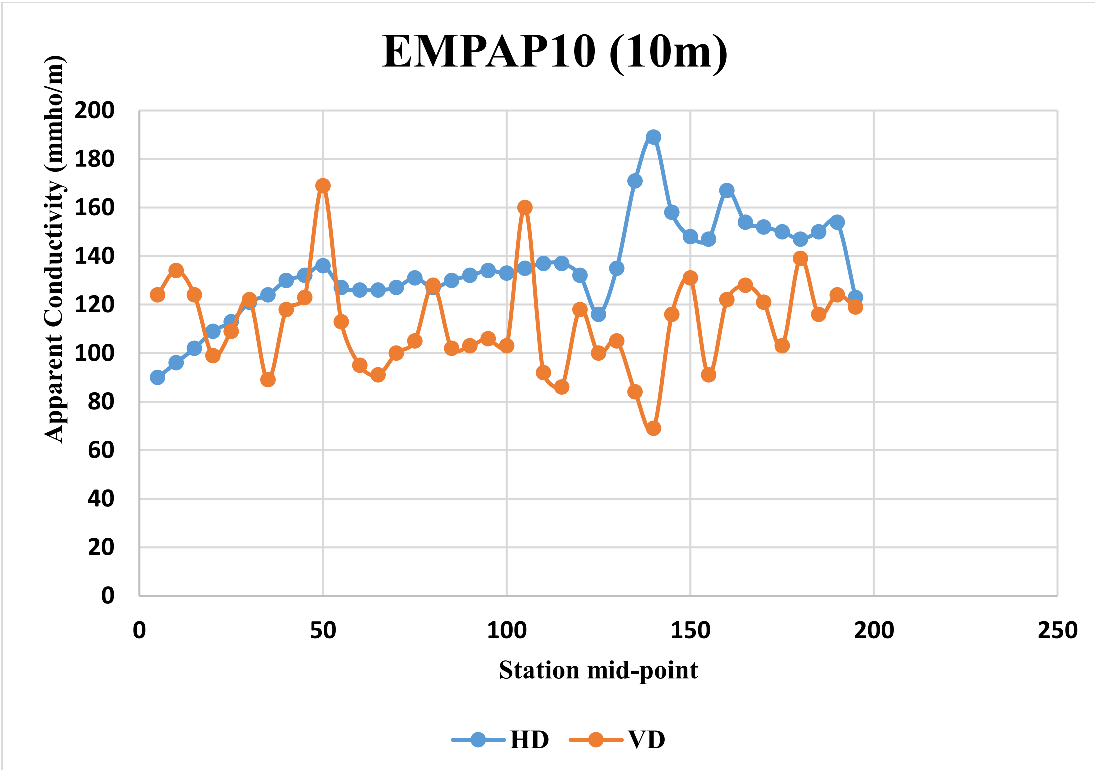
EMPAP10 (10m)
Apparent Conductivity (mmho/m)
200
180
160
140
120
100
80
60
40
20
0
0
50
100
150
200
250
Station mid-point
HD
VD

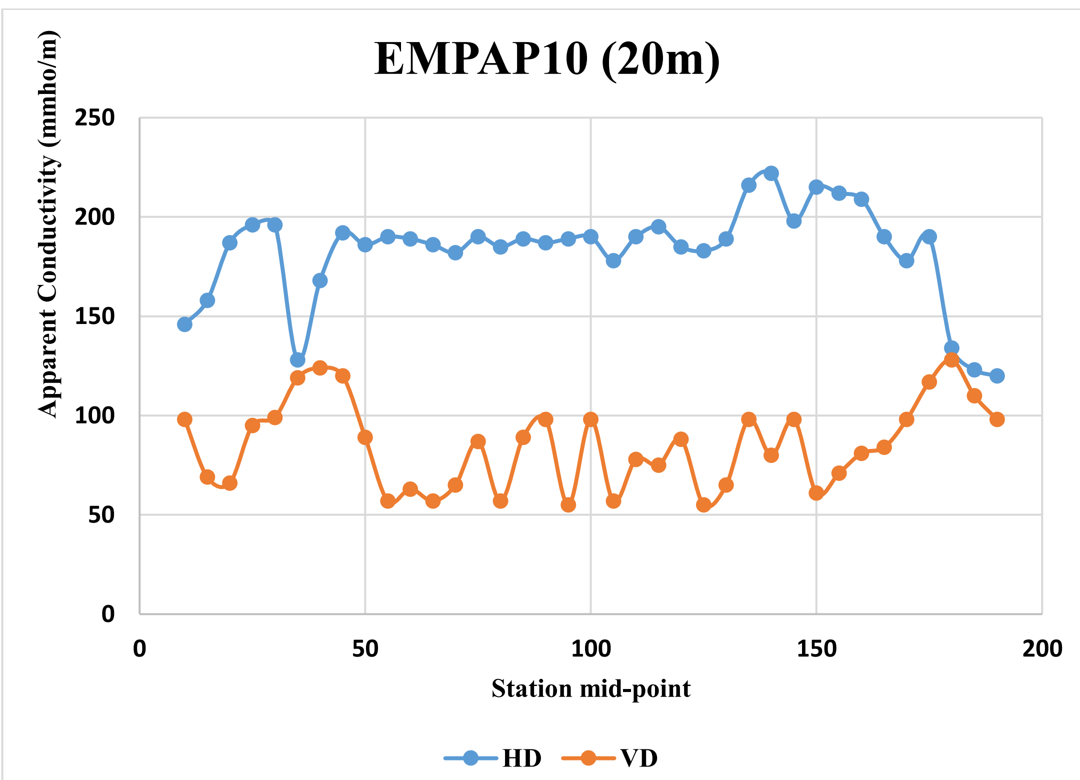
EMPAP10 (20m)
Apparent Conductivity (mmho/m)
250
200
150
100
50
0
0
50
100
150
200
Station mid-point
HD
VD

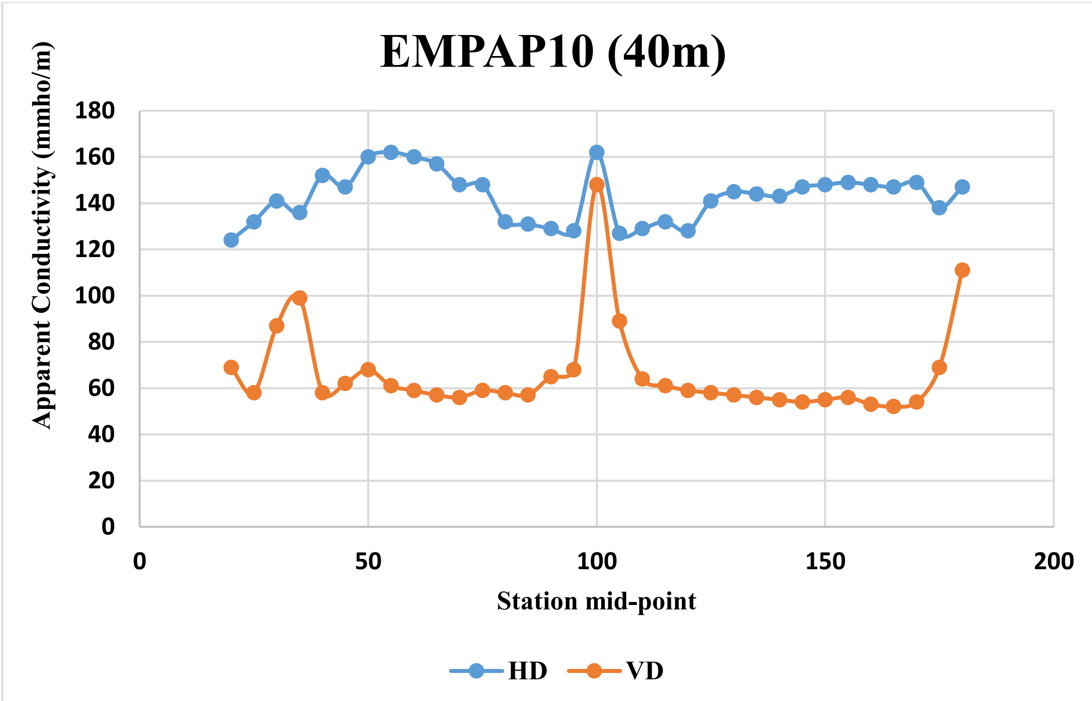

Figure 16: Plot and Values of Apparent and Real Conductivity of Horizontal Dipole Orientations along Papalanto Traverse 5 (Profile 10)

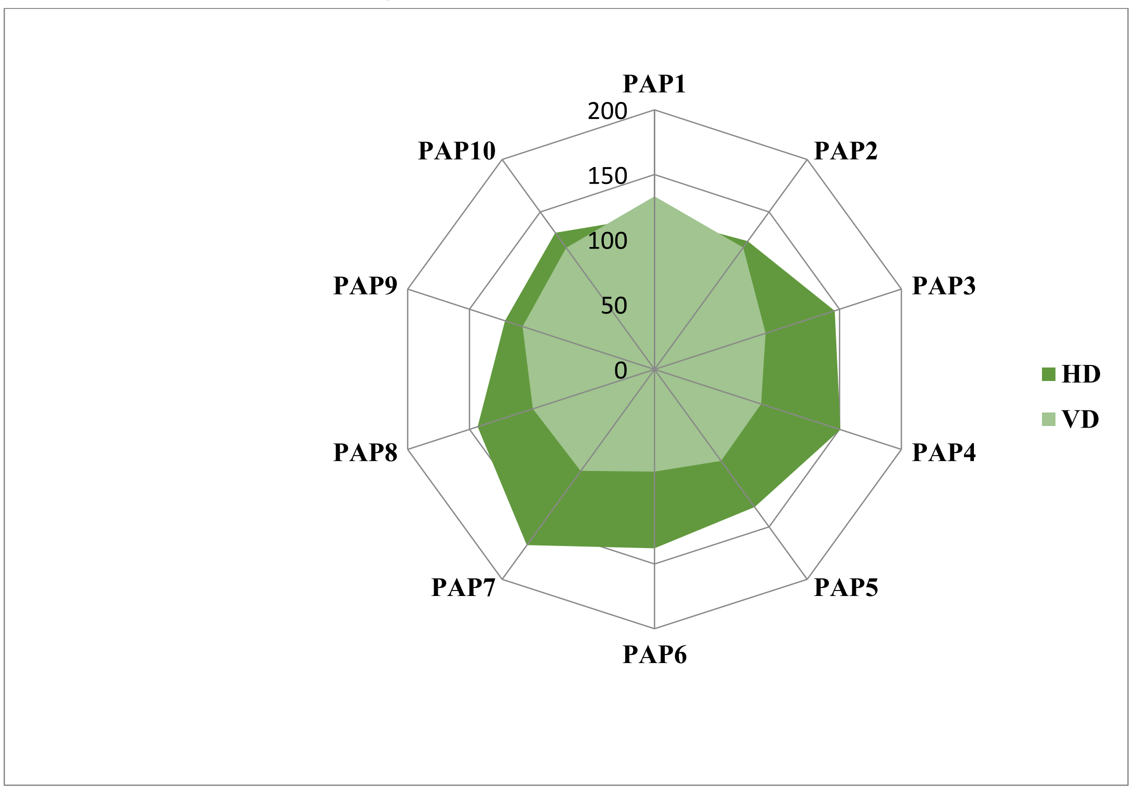

Figure 17: Distribution of Papalanto subsurface conductivity Profile for 1st Layer

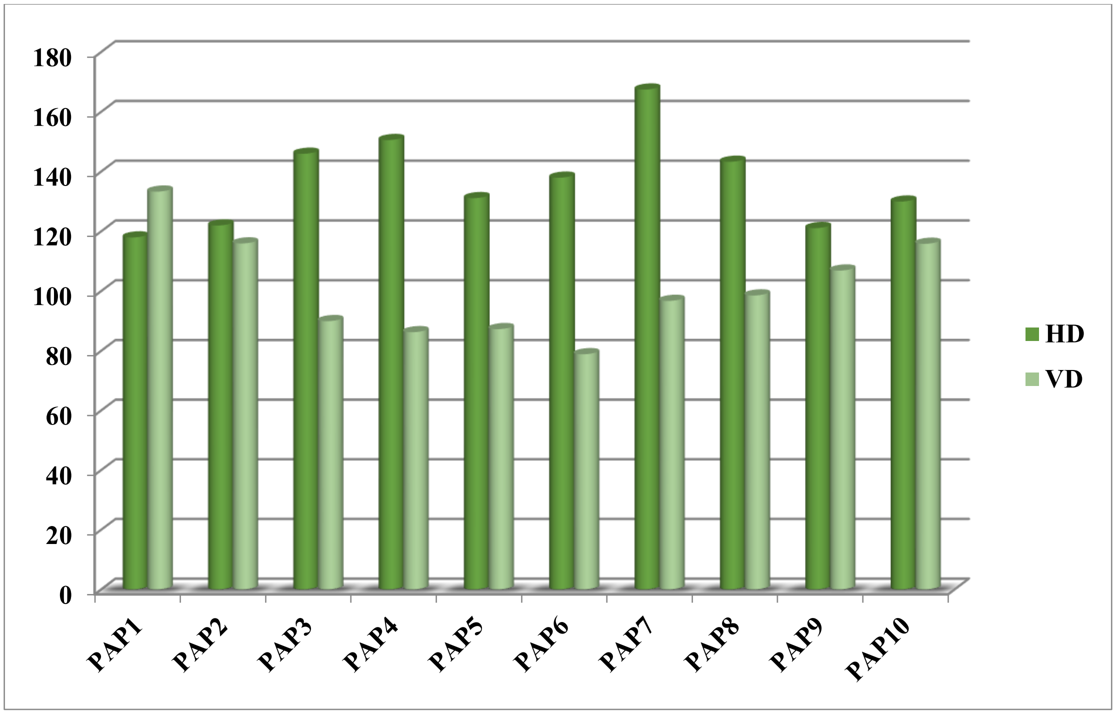

Figure 18: Papalanto subsurface Conductivity Profile variation for 1st Layer

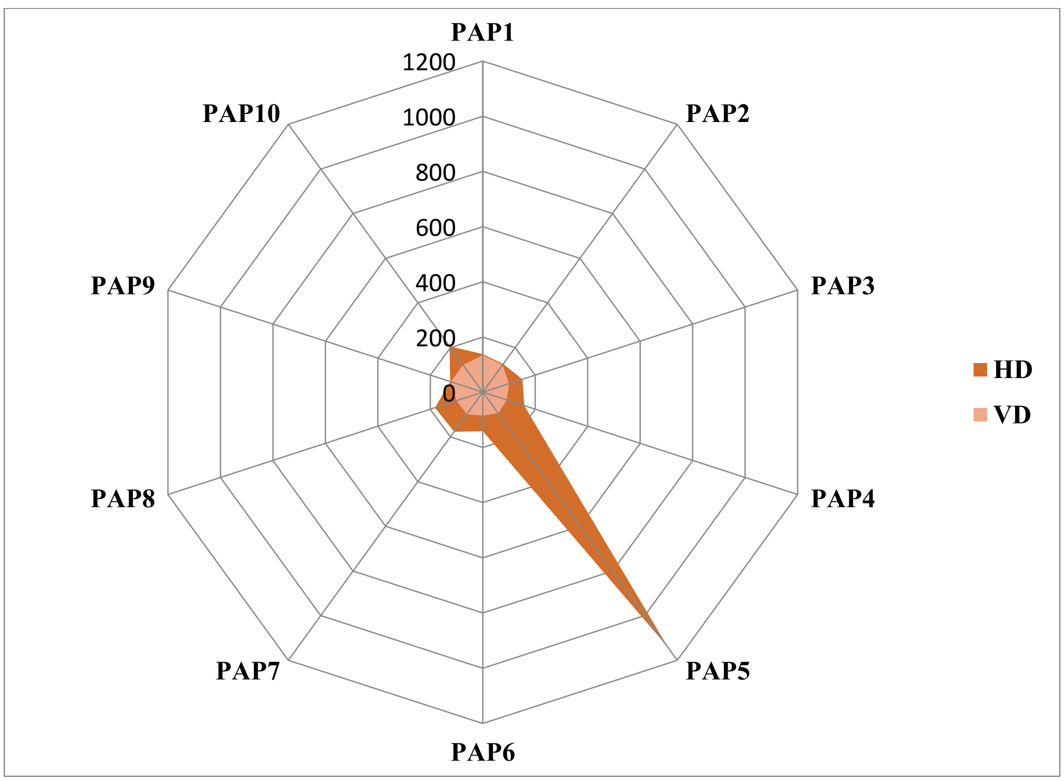

Figure 19: Distribution of Papalanto subsurface conductivity Profile for 2nd Layer

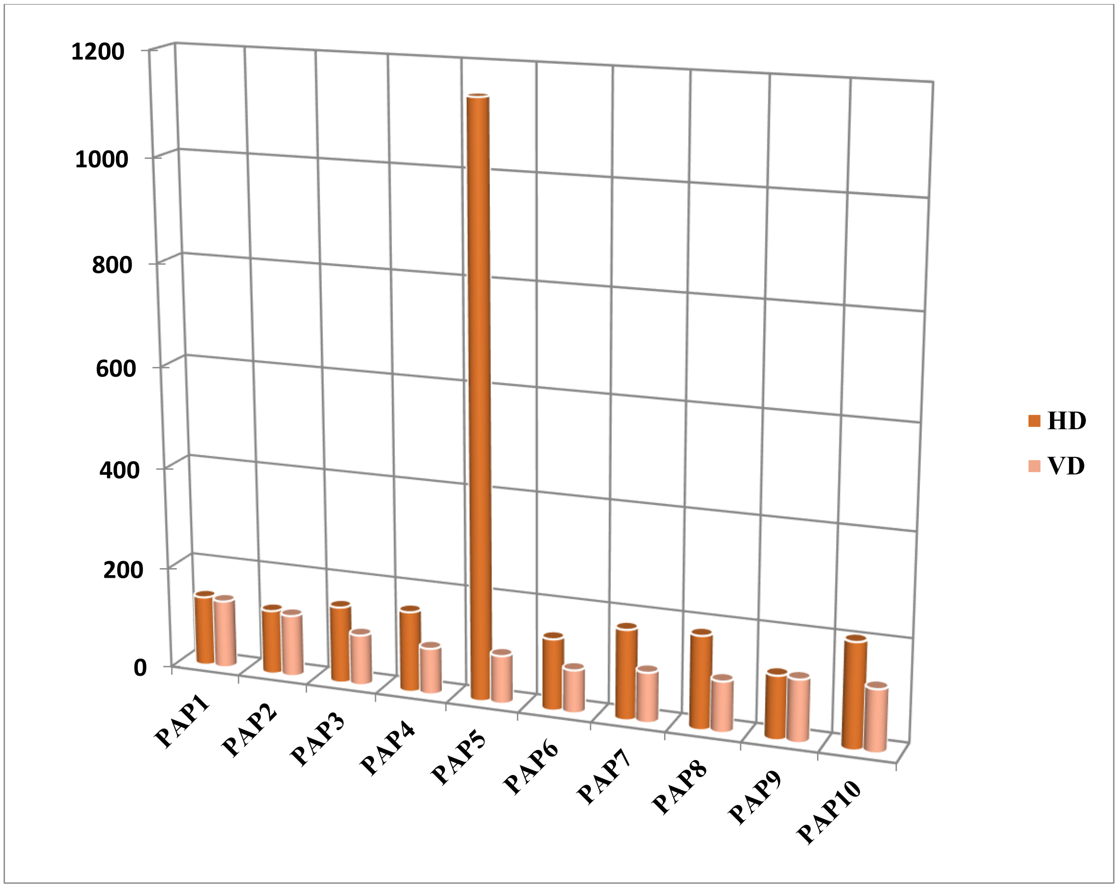

Figure 20: Papalanto Subsurface Conductivity Profile variation for 2nd Layer

CONCLUSION

Geophysical survey involving electromagnetic profiling carried out in Papalanto Districts provided preliminary information on subsurface conductivity variation for detection of possible fracture in a typical sedimentary section of South-West Nigeria. Interpretation of the EM profiles identified some conductive zones that serve as priority location for depth for further subsurcace investigation and consequent drilling for groundwater sources. The varying calculated true conductivity values were consequently recorded with the corresponding depth values in all the investigated profiles in the study area both for the horizontal and vertical dipole orientations for the first layer and the second layer. 1141.92 mmho/m was recorded as the highest true conductivity value for the Horizontal Dipole in the second layer; this occurred in Profile EMPAP5 while the highest true conductivity value for the Vertical Dipole in the first layer was 134.31 mmho/m which occurred in Profile EMPAP1. The appreciable variation in conductivity with recognizable positive peaks and broad bowl shaped anomalies observed in the high conductivities in both orientations HDM and VDM orientations is a resultant effects of weathering of the subsurface geological horizon in the study locations and are possible indications of the vulnerability of its subsurface hydrogeological environment to invasion of contaminant seepages and consequent possible pollution of the investigated locations of the study area. Sites with higher electromagnetic anomaly (high positive peaks) can be expected to be aquifers, implying locations suitable for the development of groundwater resources (Ugwu, and Nwosu, 2009). Analysis of the geophysical survey data revealed that the study area could play a significant role in providing adequate portable water for the rural dwellers. However, air- filled, altered or fissured bedrock, or predominantly clayey regolith may sometimes exhibit such anomalies. The above indicates a probable zone of thick overburden with primary to secondary fractured aquifer system with a great depth extent. In this study, data from the geophysical investigation has provided qualitative information on the hydrogeologic framework and subsurface disposition of major aquifer units in the study area. Based on the results obtained from this survey, it can be concluded that integration of electromagnetic profiling is not efficient enough to determine the groundwater potential in the study area as it can only provide qualitative interpretation. It is, however, recommended that more advanced and composite geophysical and other hydrogeological investigation tools such as aerial remote sensing, seismic refraction, electrical resistivity tomography and reflection seismology for groundwater, should be deployed in further hydogelogical studies of the area.

REFERENCES

Alabi, A.A., Ganiyu, S.A., Idowu, O.A., Ogabi, A.K., and Popoola, O.I. (2021). Investigation of Groundwater Potentials using Integrated Geophysical Methods in Maloko-Asipa, Ogun-State. *Applied Water Sciences.* 11(70): 21. https://doi.org/10.1007/s13201-021-01388-3.

Alisa A. (1990). "Telluric Current" A Dictionary of Earth Sciences Ed. Oxford University Press.

Aly, S.A., Faraq, K.S.I., Atya, M.A., and Badr, M.A.M. (2018). The Use of electromagnetic –terrain Conductivity and DC-resistivity Profiling Techniques for Bedrock Characterization at the 13th of May City Extension, Cairo Egypt. NRIAG *Journal of Astronomy and Geophysics.* 7(1): 107-122. https://doi.org/10.46717/igj.56.k.18ms.2023.3.29

Amadi, U.M.P. and S.I. Nurudeen, (1990). Electromagnetic Survey and the Search for Groundwater in the Crystalline Basement Complex of Nigeria. *Journal of Mining and Geology*, 26(1): 45-53.

Ariyo, S.O. (2007). Hydro-geophysical Investigations for Groundwater at Atan/Odosenbora Area, Southwestern Nigeria. *Ife Journal of science*. l9 (1): 87-92.

Ariyo, S.O., G.O. Adeyemi, and A.O. Oyebamiji. (2009). "Electromagnetic VLF Survey for Groundwater Development in a Contact Terrain: A Case Study of Ishara-remo, Southwestern Nigeria". *Journal of Applied Sciences Research.* 5(1): 1239– 1246.

Azmy, E.M., A.K El-Weir., A.Helaly and Faraq, K.S.I. (2023). Joint Electromagnetic Terrain Conductivity and DC-Resistivity Survey for Bedrock and Groundwater Characterization at New Al-Obour City, Egypt. (2023). Iraqi Geological Journal. 56(1): 762-776. https://doi.org/10.1016/j.nrgjag.2018.03.005

Beeson, S. and C.R.C. Jones, (1988). The Combined EMT/VES Geophysical Methods for Sitting Boreholes. *Groundwater,* 26(1): 54-63.

Billman, H.G. (1992). Offshore Stratigraphy and Paleontology of the Dahomey (Benin) Embayment, West Africa, 1st. NAPE Bull. 7(2): 121 – 130.

De-Jong, S.J., F.J.H. Dirks, A. Kikietta, G.J. Palacky and I.L. Ritsema (1981). Experimentations de methods electromagnetiques appliqués a la rechierche des eaux, souterraines en terrain de sode cristallin en Hautte Volta. Bulletin comite interafrica d' etudes hydrauliques (C.I E.H.) hydrogeology, 44(1): 17-26.

Egwebe, O., Aigbedion, I., and Ifedili, S.O. (2004). A Geo-electric Investigation for Groundwater at Ivbiaro Ebesse; Edo State: Nigeria. *Journal of Applied Science*. 22(1): 146-150.

GEONICS. (1990). EM-34 user's manual, GEONICS Ltd., Canada. 3

Hazell, J.R.T., C.R. Cratchley and A. M. Preston, (1988). The Location of Aquifers in Crystalline Rocks and Alluvium in Northern Nigeria using Combined Electromagnetic and Resistivity Techniques. *Quarterly Journal of Engineering Geology*. 21(1): 59- 175.

Huang, X., Tang, J., X. Xiao., Jiang, Q., Yang, Z., and Hu, S. (2022). A Novel Apparent Resistivity for Land –based Controlled Source Electromagnetism. Journal of Geophysics and Engineering. 9(3): 562-577. https://doi.org/10.10.93/jge/gnacl37

Ishola S.A., Makinde V., Aina J.O., Ayedun H., Akinboro F.G.,Okeyode I.C., Coker J.O., and Alatise O.O (2016). Aquifer Protection Studies and Groundwater Vulnerability Assessment in Abeokuta South Local Government Area, South-West Nigeria, *Journal of Nigerian Association of Mathematical Physics.* 33(2): 347-362.

Ishola S.A. (2019). Characterization of Groundwater Resource Potentials using Integrated Techniques in Selected Communities within Ewekoro Local Government Area South-West Nigeria. Department of Physics, FUNAAB Ph.D Thesis.

Ishola S. A, Makinde, V, Mustapha, A.O, Gbadebo, A.O, Ganiyu, S; Aluko, T. J and Ayedun, H. (2021). Integrated Hydrogeophysical and Biogeochemical Characteristics of Groundwater Sources in Ewekoro Communities, Area South-West Nigeria. *Science and Technology.* 5(12): 6-9. www.scientechpub.org

Jones H.A, Hockey R.D (1964). The Geology of Parts of Southwestern Nigeria. *Geological Survey of Nigeria*. Bull. 31(2): 22 – 24.

Kearey, P., and Brooks, M. (2002). An Introduction to Geophysical Exploration, Blackwell, pp 201.

Kehinde-Phillips, T. Ogun (1992). State maps, In: Onakomaya, S.O., K. Oyesiku and Jegede, (1992). Ogun State in Maps. Rex Charles Publishers, Ibadan. 187.

MacDonald, A., Davies, J., Calow, R., and Chilto, J. (2005). Developing Groundwater, A Guide for Rural Water Supply. 1- 358. www.itdgppublishing.org.uk

McNeill, J. D. 1980b. Technical Note: TN-6. Electromagnetic Terrain Conductivity Measurements at Low Induction Numbers. Ontario. Canada. 1-15.

McNeill, J. D. (1990). Use of Electromagnetic Methods for Groundwater Studies, in Geotechnical and Environmental Geophysics, edited by S. Ward, *Society of Exploration Geophysicists, Investigations in Geophysic*s. 5: 191– 218.

Okafor, P. and Mamah. L. (2012). "Integration of Geophysical Techniques for Groundwater Potential Investigation in Katsina-Ala, Benue State, Nigeria". *Pacific Journal of Science and Technology*. 13(2): 463-474. http://www.akamaiuniversity.us/PJST.htm

Okosun, E.A. (1998). Review of the early Tertiary Stratigraphy of Southwestern Nigeria, Nig. *Journal Mining and Geology.* 34(1):27–35.

Okpoli, C.C and Ozomoge, P. (2019). Groundwater Exploration in a Typical Southwestern Basement Terrain. *NRIAG Journal of Astronomy and Geophysics*. 9(1): 289–308. https://doi.org/10.1080/20909977.2020.1742441

Oladeji B.O (1992). Environmental Analysis of Ewekoro Formation at the Shagamu Quarry. Nig. Journal Mining and Geology. 28(1): 148–156.

Olayinka, A.I. (1990). Electromagnetic Profiling and Resistivity Soundings in Groundwater Investigation near Egbeda Kabba and Kwara State.

Olayinka, A.I., S.A. Amidu and M.A. Oladunjoye. 2004. Use of Electromagnetic Profiling and Sounding For Groundwater Exploration in the Crystalline Basement Area of Igbeti, Southwestern Nigeria. *Global Journal of Geological Science*. 2(2): 243-253.

Olorunfemi, M.O., Ojo, .J.S. Olayinka, A.I. and Mohammed, M.Z. (2001). Geophysical Investigation of Suspected Springs in Ajegunle-Igoba, near Akure, Southwestern Nigeria. *Global Journal at Pure and Applied Sciences*. 7(2): 311-320.

Omatsola, M. E, Adegoke, O. S (1981). Tectonic Evaluation and Cretaceous Stratigraphy of the Dahomey Basin. Nig. Journal Mining and Geology. 5(2): 78-83.

Omosuyi, G.O., A. Adeyemo and A.O. Adegoke. (2007). Investigation of Groundwater Prospect using Electromagnetic and Geoelectric Sounding at Afunbiowo, near Akure, Southwestern Nigeria. *Pacific Journal of Science and Technology*. 8(2): 172-182.

Onwuegbuchulam C.O.,Ikoro D. O., Nwugha V.N. , Okereke,C. N. (2016). Application of Very Low Frequency-Electromagnetic (VLF-EM) Method to Map Fractures/Conductive Zones in Auchi South western Nigeria. *The International Journal of Engineering and Science*. 5(5): 7-13. www.theijes.com

Palacky, G.J., I.L. Ritsema and S.J. De-Jong, (1981). Electromagnetic Prospecting for Groundwater in Precambrian Terrains in the Republic of Upper Volter. *Geophysical Prospecting*. 29(1): 932-955.

Tyoh, A.A., Ajegana-Idemodia, E.A., Lucky-Muhammad, M. (2025). Electromagnetic Methods. 2025 Conference of the Institute of Geosciences and Earth Resources, NSUK. https://doi.org/10.13140/RG.2.2.34257.85606

Ugwu, S. A., and Nwosu, J. I. (2009). Detection of Fractures for Groundwater Development in Oha-Ukwu using Electromagnetic Profiling. *J.App. Sci. Environ. Manage.* 13 (4) 59-63.

Vogelsang, D. (1995). Environmental Geophysics, a Practical Guide, *Springer Verlag*, 1995

WAPCO. (2000). Environmental Audit Report of the West African Portland Cement Plc, Ewekoro and Shagamu Quarries Submitted To the Federal Ministry of Environment, Abuja by the West African Portland Cement Plc, Elephant House, Alausa-Ikeja Lagos, Nigeria. 150-155.

Worthington, P.R. 1977. "Geophysical Investigations of Groundwater Resources in the Kalahari Basin". *Geophysics*. 42(4): 838-849.